

AD-A169 743

THE BUCKLING AND VIBRATION OF COMPOSITE PLATES USING

1/2

THE LEVY METHOD CONS (U) AIR FORCE INST OF TECH

WRIGHT-PATTERSON AFB OH SCHOOL OF ENGI

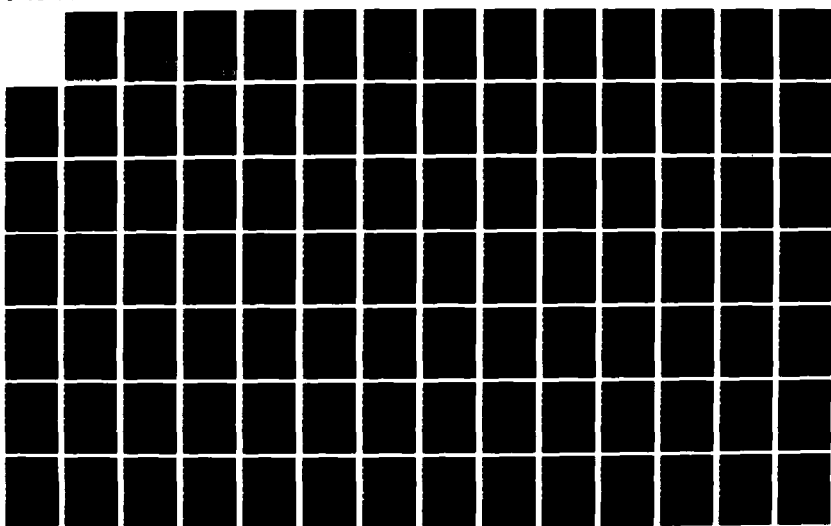
R F PALARDY

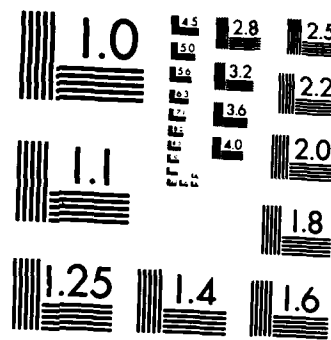
UNCLASSIFIED

DEC 87 AFIT/GAE/AR/87D-16

F/G 11/4

ML



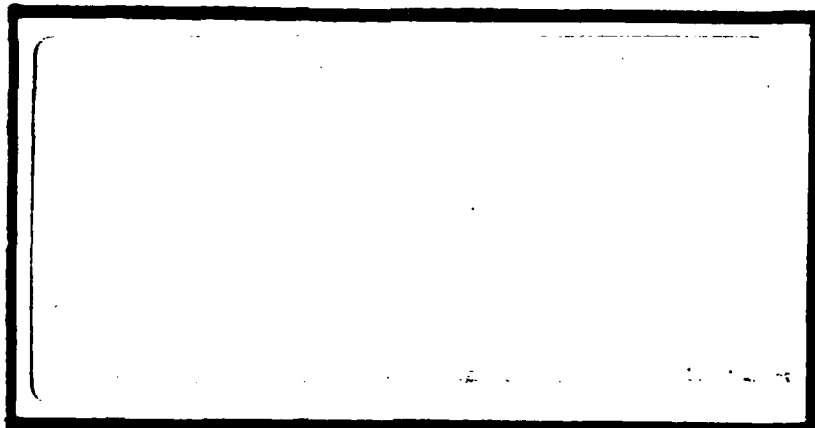


MICROCOPY RESOLUTION TEST CHART
NATIONAL BUREAU OF STANDARDS-1963-A

DTIC FILE COPY

1

AD-A189 743



DTIC
SELECTED
MAR 03 1988
S H

DEPARTMENT OF THE AIR FORCE
AIR UNIVERSITY
AIR FORCE INSTITUTE OF TECHNOLOGY

Wright-Patterson Air Force Base, Ohio

DISTRIBUTION STATEMENT A

Approved for public release
Distribution Unlimited

88 3 01 04 9

AFIT/GAE/AA/87D-16

THE BUCKLING AND VIBRATION OF COMPOSITE
PLATES USING THE LEVY METHOD CONSIDERING
SHEAR DEFORMATION AND ROTARY INERTIA

THESIS

Real F. Palardy

AFIT/GAE/AA/87D-16

Approved for public release; distribution unlimited

①
DTIC
ELECTE
MAR 03 1988
S - H D

THE BUCKLING AND VIBRATION OF COMPOSITE
PLATES USING THE LEVY METHOD CONSIDERING
SHEAR DEFORMATION AND ROTARY INERTIA

THESIS

Presented to the Faculty of the School of Engineering
of the Air Force Institute of Technology
Air University
In Partial Fulfillment of the
Requirements for the Degree of
Master of Science in Aeronautical Engineering

Real F. Palardy, B.Eng.

CAF

December 1987

Approved for public release; distribution unlimited

Table of Contents

	<u>Page</u>
Acknowledgements	ii
List of Figures	iii
List of Tables	v
List of Symbols	vi
Abstract	viii
I. Introduction	1
Background	1
Objective	3
Approach	4
II. Theory and Development of Problems	6
Anisotropic Thick Plate Theory	6
Levy Technique	21
Application of Levy Technique to Anisotropic Laminated Plate	23
Stability Problem	26
Vibration Problem	34
Formulation of Transcendental Equations	39
Simply-Supported Boundary	39
Clamped Boundary	41
Simple-Clamped Boundary	42
Simple-Free Boundary	43
Clamped-Free Boundary	44
Free-Free Boundary	45
III. Discussion and Results	48
Computer Programs	48
Analysis Performed	49
Laminated Composite Plate Properties	50
Characteristics of Levy Technique	53
Analysis of Shear Deformation and Rotary Inertia Buckling Problem	57
Vibration Problem	70
IV. Conclusions	79
Appendix A: Expression for $\det[A_{ij}]$. Buckling Problem	82
Appendix B: Expression for $\det[A_{ij}]$. Vibration Problem	84
Appendix C: Stiffness Element Determination Computer Program	86

	<u>Page</u>
Appendix D: Computer program to calculate Buckling Load or Natural Frequency of Specially Orthotropic Plate	89
Appendix E: Flowchart of Incremental Search Technique	102
Bibliography	103
Vita	105



Accession For	
NTIS GRA&I	<input checked="" type="checkbox"/>
DTIC TAB	<input type="checkbox"/>
Unannounced	<input type="checkbox"/>
Justification	
By _____	
Distribution/ _____	
Availability Codes	
Dist	Avail And, Or Special
A-1	

Acknowledgements

I would like to thank Dr. Anthony Palazotto for his unflailing support, guidance, timely suggestions, professional expertise and above all friendship throughout the nine long months it took to prepare this thesis. I would also like to thank the members of my committee, Dr. Peter Torvik and Major Lanson Hudson, for some useful comments and criticisms during my presentations.

Finally, I save my largest thank you for the person who kept reminding me that I would overcome all my problems and succeed and who kept things interesting this last year, my girlfriend and good friend, Miss Deborah Almashy. Her love, concern and the sacrifices she made this last year reminded me of the proper outlook one should always try and have when things aren't going as expected; a positive one.

List of Figures

Figure		Page
2.1	Definition of Coordinate System for Lamina	6
2.2	Definition of Coordinate System for Plate	12
2.3	Geometry of Laminate Consisting of N Lamina	14
2.4	Moment and Shear Resultants on Plate	17
3.1	Plot of Normalized Buckling Load vs Thickness Ratio for Simple-Simple Boundaries	59
3.2	Plot of Normalized Buckling Load vs Thickness Ratio for Clamped-Clamped Boundaries	60
3.3	Plot of Normalized Buckling Load vs Thickness Ratio for Simple-Clamped Boundaries	62
3.4	Plot of Normalized Buckling Load vs Thickness Ratio for Simple-Free Boundaries	64
3.5	Plot of Normalized Buckling Load vs Thickness Ratio for Clamped-Free Boundaries	65
3.6	Plot of Normalized Buckling Load vs Thickness Ratio for Free-Free Boundaries	66
3.7	Plot of Frequency vs Thickness Ratio for Simple-Simple Boundaries	71
3.8	Plot of Frequency vs Thickness Ratio for Clamped-Clamped Boundaries	72
3.9	Plot of Frequency vs Thickness Ratio for Simple-Clamped Boundaries	74

Figure		Page
3.10	Plot of Frequency vs Thickness Ratio for Simple-Free Boundaries	75
3.11	Plot of Frequency vs Thickness Ratio for Clamped-Free Boundaries	76

List of Tables

Table		Page
3.1	Stiffness Parameters for a One Inch Thick Plate	51
3.2	Stiffness Parameters for a Two Inch Thick Plate	52
3.3	Comparison of Galerkin and Levy Techniques for a Plate Simply-Supported on All Four Edges. Plate Thickness is One Inch	54
3.4	Natural Frequency of a Two Inch Thick Plate With and Without Rotary Inertia. Simple-Clamped Boundaries in Y	56
3.5	Comparison of Discrepancies Between Shear Deformation Theory and Classical Plate Theory for Stability Problems	67
3.6	Comparison of Discrepancies Between Shear Deformation Theory and Classical Plate Theory for Vibration Problems	78

List of Symbols

a	plate x dimension
A^*, B^*, C^*	general constants in displacement functions
A_i, B_i, C_i	constants in displacement functions
A_{ij}	extensional stiffnesses
b	plate y dimension
D_{ij}	bending stiffnesses
E_i	Young's Modulus in the i direction
G_{ii}	Shear modulus in the i-j plane
g_c	32.174 ft/sec ²
h	plate thickness
I	mass moment of inertia
k	Mindlin's shear deformation correction factor
K	midplane curvatures
m	integer describing number of symmetric layers in laminate
n	integer determining mode of the problem
M_x, M_y, M_{xy}	moments
N_x, N_y	axial forces
N	simplified form for m/a
Q_{ij}	reduced stiffnesses
$\bar{Q}_{ij}, \bar{Q}_{ij}'$	transformed reduced stiffnesses
S	plate length to thickness ratio
S_{ij}	compliance values
u, v, w	displacements
W(y)	displacement in z direction
x, y, z	plate geometrical axes

1,2,3	laminae principal axes
ϵ_i	strain components
θ	fiber orientation angle
α, β, γ	variables describing magnitude of displacements
$\Lambda(\theta), \tilde{\Lambda}(\theta)$	proportionality functions for stability problem
$\Omega(\theta), \tilde{\Omega}(\theta)$	proportionality functions for vibration problem
ψ_i	rotations due to bending
π	3.1415927
ρ	density
σ_i	stress components
ν_{ij}	Poisson's ratio between i and j directions
v_i	functions of α, β, γ
ω	natural frequency
ς	parameter describing magnitude of displacements

ABSTRACT

An analytical study is conducted to determine the stability and free vibration characteristics of laminated anisotropic plates using the Levy approach. Included in the plate model are the effects of shear deformation and rotary inertia. Six different boundary conditions in the y direction are analyzed in conjunction with simply-supported boundaries in the x direction. The y directed boundaries considered are simple-simple, clamped-clamped, simple-clamped, simple-free, clamped-free and, free-free.

Solutions are presented for the buckling loads and natural frequencies of rectangular, graphite-epoxy symmetric plates. The results indicate the importance of including shear effects and rotary inertia in a plate's mathematical model. The overall importance of these equation parameters is definitely a function of the boundary condition and a general statement cannot be made. In addition, the effectiveness of the Levy technique, in studying laminated problems, becomes apparent in handling the more complicated boundaries as compared to the Galerkin or Rayleigh-Ritz techniques.

I. Introduction

Background

The use of composite material in many varied industries has increased tremendously in the past several years. This is largely due to the high strength to weight ratios of composites as well as their ability to be tailored to meet design requirements of strength and stiffness. A special interest is the use of composite materials in aircraft structures.

Coinciding with these new applications is the need to better understand the physical and dynamic responses of the composites to complex in-plane stress systems [7]. Past research has clearly indicated the need for a refinement of the classical plate theory (CPT) in order to better predict composite plate behaviour. The assumption that plane sections remain plane after deformation (Kirchhoff hypothesis) results in a mathematical model of plate behaviour which is overstiff [7]. The need to include through-the-thickness shear effects was first recognized by Reissner [14]. Mindlin, shortly thereafter, added the thickness-dependent effects of rotary inertia, for the vibration problem, in his mathematical model for the flexual motion of isotropic plates [10]. Mindlin's two dimensional theory is based on the premise that plate displacement is a result of two rotations due to bending and two rotations due to shear deformation. Furthermore, no warping of the plane sections is assumed. This inconsistency is somewhat corrected by the introduction of a correction factor [2].

Yang, Norris, and Stavsky [1] used Mindlin's model to develop the frequency equations for the propagation of harmonic waves in an infinite, two-layer isotropic plate. Their theory (referred to as YNS theory) was applied by Whitney and Pagano [12] to laminated plates consisting of an arbitrary number of bonded anisotropic layers, each having one plane of material symmetry parallel to the central plane of the plate. Their study [12] centered on solving for the vibrations of antisymmetric angle-ply plate strips. Work by Brunelle [1] on transversely isotropic Mindlin plates considered the stability of rectangular plates simply-supported on a pair of opposite edges and carrying uniaxial membrane compression [24]. This work is one of the earliest to consider the feasibility of applying Levy's technique [13] to composite plates and thereby obtain a solution for displacement that is not modelled as a double series expansion. The accuracy of the expression for displacement is not dependent on the number of terms retained from the expansion in this case. This type of solution is commonly referred to as a closed-form solution.

Refinement of finite element analysis with the inclusion of transverse shear effects began with the work of Pryor and Barker [25]. They studied the cylindrical bending of symmetric cross-ply laminates using a model based on Reissner plate theory. YNS theory was modelled by Reddy [18] in his study of the free vibrations of antisymmetric angle-ply plates. His later work [18] considered orthotropic laminates of bimodulus materials. A different approach was used by Sathyamoorthy and Chia [20] in their study of anisotropic skew plates. They applied Von Karman's non-linear plate equations to calculate the large amplitude vibrations of the skew plates.

More recent work by Dawe and Craig [6,7,16] has investigated the effects of shear deformation in a number of plate vibration and stability problems. In each case, the Rayleigh-Ritz or finite-strip methods were used to generate numerical results. Bowlus [2] analyzed the vibration characteristics of anisotropic laminated plates, with shear deformation and rotary inertia, using the Galerkin method. Reddy's latest work [26] applies the Levy technique to the bending problem of symmetrically laminated rectangular plates. His model includes shear deformation and considers two different plates, a single layered orthotropic plate, and a three layered cross ply composite plate. His numerical results are generated by a solution based on the state-space concept developed by Franklin in 1968.

Thus, the literature does not indicate any closed form solutions for the m -layered symmetric laminates where both shear deformation and rotary inertia effects have been considered with application to plate buckling and plate vibration respectively.

Objectives

There are three main objectives to this thesis. First, the effectiveness of the Levy technique in calculating natural frequencies and buckling load for anisotropic laminated plates is determined. The plate's mathematical model includes shear deformation through the thickness and rotary inertia. Second, the technique is used to evaluate "baseline" solutions for some of the boundary conditions which are extremely difficult to analyze using the approximate methods based on energy principles. Finally, comparison with classical solutions, when available, are used to determine the importance of shear effects and rotary inertia in the plate model.

Approach

A direct approach is followed to successfully realize the stated objectives. The motion of the laminated plate is modelled using YNS theory [11]. Solution of the derived coupled partial differential equations of motion is obtained by application of the Levy technique. The plate studied in this thesis, a specially - orthotropic laminate, does not contain bending-extensional or bending-twisting coupling terms. From the equations of motion, displacement functions are evaluated and used to solve the boundary value problem (BVP) defined by the application of specific boundary conditions. Simplification of the BVP leads to a transcendental equation for either the natural frequency or the buckling load, depending on the problem under consideration. A computer program is written, in Fortran 77, to solve the transcendental equation using the incremental search method [5]. Limits to the effectiveness of the Levy technique are then evaluated in terms of allowable laminates and plate geometries/size.

The boundary conditions always have a set of simple supports in one direction with the other direction consisting of either simple-simple, clamped-clamped, simple-clamped, simple-free, clamped-free, or free-free. Comparisons of results to classical solutions and solutions obtained using the various energy techniques are presented whenever available. The importance of shear deformation and rotary inertia is determined by calculating the natural frequencies and buckling loads over a range of length to width and length to thickness ratios. Initially, rotary inertia is neglected in order to better understand the relative significance of considering shear deformation effects. Rotary inertia is then re-introduced into the vibration plate model and

calculations are repeated, thereby providing an indication of its importance in the accurate modelling of thick plates.

II. Theory and Modelling

Anisotropic Thick Plate Theory

Classical Laminated Plate Theory (CLPT) incorporates constitutive relationships for an orthotropic lamina through the plate thickness resulting in expressions which approximate force resultants in terms of displacement functions. This theory provides concepts which are required in the subsequent development of the equations of motion. As a starting point, the basic constitutive relationships for an individual lamina are developed [2]. One should refer to reference [17] for a more complete and detailed derivation of these relations.

The basic constitutive relationships for a single orthotropic layer in the fiber oriented reference system, as described by figure 2.1, are

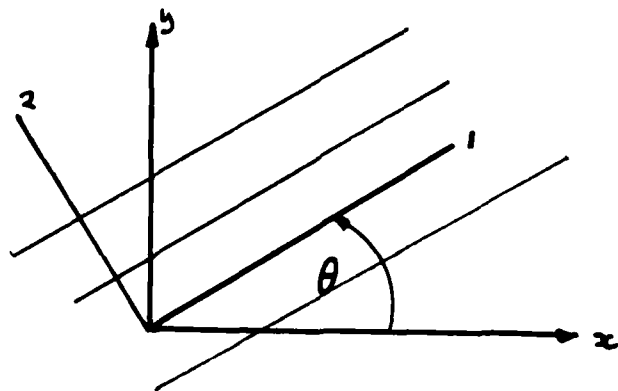


Figure 2.1. Definition of Coordinate System

$$\left\{ \begin{array}{l} \epsilon_1 \\ \epsilon_2 \\ \epsilon_3 \\ \epsilon_4 \\ \epsilon_5 \\ \epsilon_6 \end{array} \right\} = \begin{bmatrix} S_{11} & S_{12} & S_{13} & 0 & 0 & 0 \\ S_{12} & S_{22} & S_{23} & 0 & 0 & 0 \\ S_{13} & S_{23} & S_{33} & 0 & 0 & 0 \\ 0 & 0 & 0 & S_{44} & 0 & 0 \\ 0 & 0 & 0 & 0 & S_{55} & 0 \\ 0 & 0 & 0 & 0 & 0 & S_{66} \end{bmatrix} \left\{ \begin{array}{l} \sigma_1 \\ \sigma_2 \\ \sigma_3 \\ \sigma_4 \\ \sigma_5 \\ \sigma_6 \end{array} \right\} \quad (1)$$

where ϵ_1 , ϵ_2 , and ϵ_3 are the normal strains, ϵ_4 , ϵ_5 , and ϵ_6 are the shearing strains, σ_1 , σ_2 , and σ_3 are the normal stresses and σ_4 , σ_5 , and σ_6 are the shearing stresses. The S_{ij} terms are compliance terms and may be written in terms of the lamina engineering constants as:

$$\begin{aligned} S_{11} &= 1/E_1 \\ S_{12} &= -\nu_{21}/E_2 \\ S_{13} &= -\nu_{31}/E_3 \\ S_{22} &= 1/E_2 \\ S_{23} &= -\nu_{23}/E_2 \\ S_{33} &= 1/E_3 \\ S_{44} &= 1/G_{23} \\ S_{55} &= 1/G_{31} \\ S_{66} &= 1/G_{12} \end{aligned} \quad (2)$$

and E_i is the Young's modulus in the i th direction, ν_{ij} is Poisson's ratio for transverse strain in the j th direction when loaded in the i th direction, and G_{ij} is the shear modulus in the $i-j$ plane.

Equation (1) may be inverted to give the relationship of stresses in terms of strain in the form

$$\{\sigma\} = [Q']\{\epsilon\} \quad (3)$$

[Q'] is referred to as the reduced stiffness matrix and has the following form:

$$[Q'] = \begin{bmatrix} Q'_{11} & Q'_{12} & Q'_{13} & 0 & 0 & 0 \\ Q'_{12} & Q'_{22} & Q'_{23} & 0 & 0 & 0 \\ Q'_{13} & Q'_{23} & Q'_{33} & 0 & 0 & 0 \\ 0 & 0 & 0 & Q'_{44} & 0 & 0 \\ 0 & 0 & 0 & 0 & Q'_{55} & 0 \\ 0 & 0 & 0 & 0 & 0 & Q'_{66} \end{bmatrix} \quad (4)$$

where

$$\begin{aligned} Q'_{11} &= (S_{22}S_{33} - S_{23}^2)/S \\ Q'_{12} &= (S_{13}S_{23} - S_{12}S_{33})/S \\ Q'_{13} &= (S_{12}S_{23} - S_{13}S_{22})/S \\ Q'_{22} &= (S_{33}S_{11} - S_{13}^2)/S \\ Q'_{23} &= (S_{12}S_{13} - S_{23}S_{11})/S \\ Q'_{33} &= (S_{11}S_{22} - S_{12}^2)/S \\ Q'_{44} &= 1/S_{44} \\ Q'_{55} &= 1/S_{55} \\ Q'_{66} &= 1/S_{66} \\ S &= S_{11}S_{22}S_{33} - S_{11}S_{23}^2 - S_{22}S_{13}^2 - S_{33}S_{12}^2 + 2S_{12}S_{23}S_{13} \end{aligned} \quad (5)$$

If the lamina is not oriented with the principal x-y axis but rather is at an angle θ (see figure 2.1), the reduced stiffness matrix must be transformed. The matrix applied to the stiffness terms to reflect the shift in the laminae axes is defined as:

$$[T] = \begin{bmatrix} l^2 & p^2 & 0 & 0 & 0 & 1p \\ p^2 & l^2 & 0 & 0 & 0 & -1p \\ 0 & 0 & 1 & 0 & 0 & 0 \\ 0 & 0 & 0 & 1 & -p & 0 \\ 0 & 0 & 0 & p & 1 & 0 \\ -2lp & 2lp & 0 & 0 & 0 & l^2-p^2 \end{bmatrix} \quad (6)$$

where $l = \cos \theta$ and $p = \sin \theta$. The transformed stiffness matrix for the lamina is represented as

$$[\bar{Q}'] = [T][Q'][T]^t \quad (7)$$

$$\text{and } \{\sigma\} = [\bar{Q}']\{\epsilon\} \quad (8)$$

where

$$[\bar{Q}'] = \begin{bmatrix} \bar{Q}_{11}' & \bar{Q}_{12}' & \bar{Q}_{13}' & 0 & 0 & \bar{Q}_{16}' \\ \bar{Q}_{12}' & \bar{Q}_{22}' & \bar{Q}_{23}' & 0 & 0 & \bar{Q}_{26}' \\ \bar{Q}_{13}' & \bar{Q}_{23}' & \bar{Q}_{33}' & 0 & 0 & \bar{Q}_{36}' \\ 0 & 0 & 0 & \bar{Q}_{44}' & \bar{Q}_{45}' & 0 \\ 0 & 0 & 0 & \bar{Q}_{45}' & \bar{Q}_{55}' & 0 \\ \bar{Q}_{16}' & \bar{Q}_{26}' & \bar{Q}_{36}' & 0 & 0 & \bar{Q}_{66}' \end{bmatrix} \quad (9)$$

In order to simplify the stress-strain relationships given by Eq(8), a state of plane stress is assumed for the laminae. That is, the individual laminae are considered to be thin enough that the average value of σ_z across the thickness is negligible [21]. Thus, from Eq. (8)

$$\begin{aligned} \sigma_z &= 0 = \bar{Q}_{13}' \epsilon_x + \bar{Q}_{23}' \epsilon_y + \bar{Q}_{33}' \epsilon_z + \bar{Q}_{36}' \gamma_{xy} \\ \text{or } \epsilon_z &= (\bar{Q}_{13}' / \bar{Q}_{33}') \epsilon_x + (\bar{Q}_{23}' / \bar{Q}_{33}') \epsilon_y + (\bar{Q}_{36}' / \bar{Q}_{33}') \gamma_{xy} \end{aligned} \quad (10)$$

If this expression for ϵ_z is substituted back into Eq (8), the resulting transformed stiffness matrix is defined as $[\bar{Q}]$ and has the form

$$[\bar{Q}] = \begin{bmatrix} \bar{Q}_{11} & \bar{Q}_{12} & 0 & 0 & \bar{Q}_{16} \\ \bar{Q}_{12} & \bar{Q}_{22} & 0 & 0 & \bar{Q}_{26} \\ 0 & 0 & \bar{Q}_{44} & \bar{Q}_{45} & 0 \\ 0 & 0 & \bar{Q}_{45} & \bar{Q}_{55} & 0 \\ \bar{Q}_{16} & \bar{Q}_{26} & 0 & 0 & \bar{Q}_{66} \end{bmatrix} \quad (11)$$

where

$$\begin{aligned} \bar{Q}_{11} &= Q_{11} \cos^4 \theta + 2(Q_{12} + 2Q_{66}) \sin^2 \theta \cos^2 \theta + Q_{22} \sin^4 \theta \\ \bar{Q}_{12} &= (Q_{11} + Q_{22} - 4Q_{66}) \sin^2 \theta \cos^2 \theta + Q_{12} (\sin^4 \theta + \cos^4 \theta) \\ \bar{Q}_{22} &= Q_{11} \sin^4 \theta + 2(Q_{12} + 2Q_{66}) \sin^2 \theta \cos^2 \theta + Q_{22} \cos^4 \theta \\ \bar{Q}_{16} &= (Q_{11} - Q_{12} - 2Q_{66}) \sin \theta \cos^3 \theta + (Q_{12} - Q_{22} + 2Q_{66}) \sin^3 \theta \cos \theta \\ \bar{Q}_{26} &= (Q_{11} - Q_{12} - 2Q_{66}) \sin^3 \theta \cos \theta + (Q_{12} - Q_{22} + 2Q_{66}) \sin \theta \cos^3 \theta \quad (12) \\ \bar{Q}_{44} &= Q_{44} \cos^2 \theta + Q_{55} \sin^2 \theta \\ \bar{Q}_{45} &= (Q_{44} - Q_{55}) \cos \theta \sin \theta \\ \bar{Q}_{55} &= Q_{55} \cos^2 \theta + Q_{44} \sin^2 \theta \\ \bar{Q}_{66} &= (Q_{11} + Q_{22} - 2Q_{12} - 2Q_{66}) \sin^2 \theta \cos^2 \theta + Q_{66} (\sin^4 \theta + \cos^4 \theta) \end{aligned}$$

and

$$\begin{aligned} Q_{11} &= E_1 / (1 - \nu_{12} \nu_{21}) \\ Q_{12} &= \nu_{12} E_2 / (1 - \nu_{12} \nu_{21}) \\ Q_{22} &= E_2 / (1 - \nu_{12} \nu_{21}) \\ Q_{44} &= G_{23} \\ Q_{55} &= G_{31} \\ Q_{12} &= G_{12} \quad (13) \end{aligned}$$

With the removal of σ_z , the stiffness matrix becomes a 5x5 matrix. The stress-strain relationships defined in Eq. 8 may be re-written in terms of normal and shear values as:

$$\begin{Bmatrix} \sigma_x \\ \sigma_y \\ \tau_{xy} \end{Bmatrix} = \begin{bmatrix} \bar{Q}_{11} & \bar{Q}_{12} & \bar{Q}_{16} \\ \bar{Q}_{12} & \bar{Q}_{22} & \bar{Q}_{26} \\ \bar{Q}_{16} & \bar{Q}_{26} & \bar{Q}_{66} \end{bmatrix} \begin{Bmatrix} \epsilon_x \\ \epsilon_y \\ \gamma_{xy} \end{Bmatrix} \quad (14)$$

and

$$\begin{Bmatrix} \tau_{yz} \\ \tau_{xz} \end{Bmatrix} = \begin{bmatrix} \bar{Q}_{44} & \bar{Q}_{45} \\ \bar{Q}_{45} & \bar{Q}_{55} \end{bmatrix} \begin{Bmatrix} \gamma_{yz} \\ \gamma_{xz} \end{Bmatrix} \quad (15)$$

These relationships are for a single lamina and may be used as a starting point in the derivation of expressions for the forces and moments existing in a laminate of N perfectly bonded lamina. Before doing so, a further simplification, dealing with ϵ_z is discussed as well as the convention followed in defining the rotations ψ_x and ψ_y .

The strain in the z -direction is assumed to be small enough as to be negligible. This inconsistency, widely accepted in plate theory, implies that no stretching occurs in the direction perpendicular to the plate midplane. For a laminate, this assumption leads to a discontinuity in ϵ_z at the lamina upper and lower boundaries, but it is very small. This assumption allows the modelling of the displacement field for the laminate with YNS theory. Thus, the plate displacements can be assumed to have the forms

$$\begin{aligned} u &= u^0(x, y, t) + z\psi_x(x, y, t) \\ v &= v^0(x, y, t) + z\psi_y(x, y, t) \\ w &= w(x, y, t) \end{aligned} \quad (16)$$

where u, v, w are the x, y , and z coordinate displacements respectively, u^0 and v^0 are the pre-stressed displacements of the laminate midplane, and ψ_x and ψ_y are rotations of lines perpendicular to the midplane due to bending [2]. It should be noted that the inconsistency mentioned earlier could be removed by including terms, which are linear and quadratic in z , to the expression for w . Reference [9] makes it clear however, that for most plates, the inconsistency is negligible.

The expressions ψ_x and ψ_y are defined as rotations about the y and x axes respectively due to bending moments. With the axis system defined in figure 2.1, the rotations indicated are produced by positive bending moments.

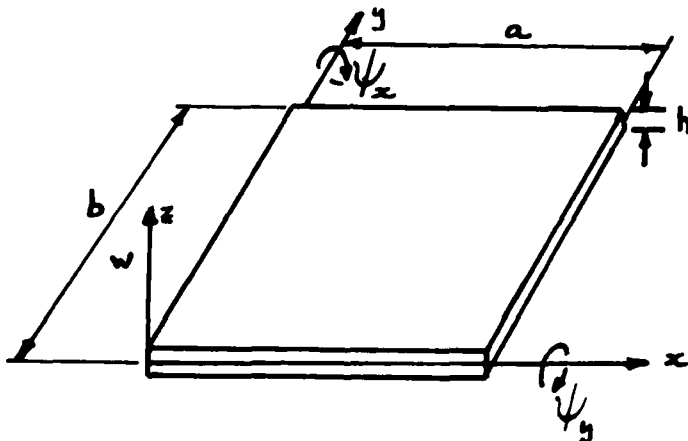


Figure 2.2. Coordinate System of Plate

For small strains, the first order engineering definitions are:

$$\epsilon_x = u_{,x}$$

$$\epsilon_y = v_{,y}$$

$$\gamma_{xy} = u_{,y} + v_{,x}$$

Substituting the displacement field given by Eq. (16) gives

$$\begin{aligned}\epsilon_x &= u^0, x + z\psi_{x,x} \\ \epsilon_y &= v^0, y + z\psi_{y,y} \\ \gamma_{xy} &= u^0, y + v^0, x + z\psi_{x,y} + z\psi_{y,x}\end{aligned}\quad (18)$$

or

$$\begin{Bmatrix} \epsilon_x \\ \epsilon_y \\ \gamma_{xy} \end{Bmatrix} = \begin{Bmatrix} \epsilon_x^0 \\ \epsilon_y^0 \\ \gamma_{xy}^0 \end{Bmatrix} + z \begin{Bmatrix} \kappa_x \\ \kappa_y \\ \kappa_{xy} \end{Bmatrix} \quad (19)$$

where the strains at the plate middle surface are

$$\begin{Bmatrix} \epsilon_x^0 \\ \epsilon_y^0 \\ \gamma_{xy}^0 \end{Bmatrix} = \begin{Bmatrix} u^0, x \\ v^0, y \\ u^0, y + v^0, x \end{Bmatrix} \quad (20)$$

and the midplane curvatures due to bending are

$$\begin{Bmatrix} \kappa_x \\ \kappa_y \\ \kappa_{xy} \end{Bmatrix} = \begin{Bmatrix} \psi_{x,x} \\ \psi_{y,y} \\ \psi_{x,y} + \psi_{y,x} \end{Bmatrix} \quad (21)$$

Eqs. (20) and (21) give expressions for the strains in terms of displacements and these may now be substituted into Eq. (14) to give the stress - displacement relationships for the k th layer of the laminate:

$$\begin{Bmatrix} \sigma_x \\ \sigma_y \\ \tau_{xy} \end{Bmatrix}_k = \begin{Bmatrix} \bar{Q}_{11} & \bar{Q}_{12} & \bar{Q}_{16} \\ \bar{Q}_{12} & \bar{Q}_{22} & \bar{Q}_{26} \\ \bar{Q}_{16} & \bar{Q}_{26} & \bar{Q}_{66} \end{Bmatrix}_k \begin{Bmatrix} u^0, x \\ v^0, y \\ u^0, y + v^0, x \end{Bmatrix} + z \begin{Bmatrix} \psi_{x,x} \\ \psi_{y,y} \\ \psi_{x,y} + \psi_{y,x} \end{Bmatrix} \quad (22)$$

Following Jones [17], the resultant forces and moments acting on the laminate are obtained by integrating the stresses in each layer through the laminate thickness. Thus, for a laminate described in figure 2.3, with N lamina, the forces and moments are:

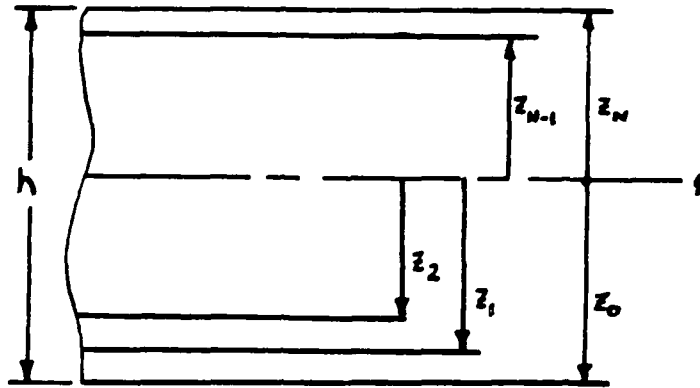


Figure 2.3. Geometry of laminate consisting of N lamina

$$(N_x, N_y, N_{xy}) = \int_{-h/2}^{h/2} (\sigma_x, \sigma_y, \tau_{xy}) dz = \sum_{k=1}^N \int_{z_{k-1}}^{z_k} (\sigma_x, \sigma_y, \tau_{xy}) dz$$

and

(23)

$$(M_x, M_y, M_{xy}) = \int_{-h/2}^{h/2} (\sigma_x, \sigma_y, \tau_{xy}) z dz = \sum_{k=1}^N \int_{z_{k-1}}^{z_k} (\sigma_x, \sigma_y, \tau_{xy}) z dz$$

These integrations may be simplified somewhat as the stiffnesses are constant within the laminae and the stresses are not functions of z . Thus, Eq. (23) may be rewritten as

$$\begin{Bmatrix} N_x \\ N_y \\ N_{xy} \end{Bmatrix} = \begin{bmatrix} A_{11} & A_{12} & A_{16} \\ A_{12} & A_{22} & A_{26} \\ A_{16} & A_{26} & A_{66} \end{bmatrix} \begin{Bmatrix} \epsilon_x^0 \\ \epsilon_y^0 \\ \gamma_{xy}^0 \end{Bmatrix} + \begin{bmatrix} B_{11} & B_{12} & B_{16} \\ B_{12} & B_{22} & B_{26} \\ B_{16} & B_{26} & B_{66} \end{bmatrix} \begin{Bmatrix} \kappa_x \\ \kappa_y \\ \kappa_{xy} \end{Bmatrix} \quad (24)$$

and

$$\begin{Bmatrix} M_x \\ M_y \\ M_{xy} \end{Bmatrix} = \begin{bmatrix} B_{11} & B_{12} & B_{16} \\ B_{12} & B_{22} & B_{26} \\ B_{16} & B_{26} & B_{66} \end{bmatrix} \begin{Bmatrix} \epsilon_x^0 \\ \epsilon_y^0 \\ \gamma_{xy}^0 \end{Bmatrix} + \begin{bmatrix} D_{11} & D_{12} & D_{16} \\ D_{12} & D_{22} & D_{26} \\ D_{16} & D_{26} & D_{66} \end{bmatrix} \begin{Bmatrix} \kappa_x \\ \kappa_y \\ \kappa_{xy} \end{Bmatrix} \quad (25)$$

where

$$A_{ij} = \sum_{k=1}^N (Q_{ij})_k (z_k - z_{k-1}) \quad (26)$$

$$B_{ij} = 1/2 \sum_{k=1}^N (Q_{ij})_k (z_k^2 - z_{k-1}^2) \quad (27)$$

$$D_{ij} = 1/3 \sum_{k=1}^N (Q_{ij})_k (z_k^3 - z_{k-1}^3) \quad (28)$$

Required now are the expressions for the shear forces on the plate in terms of displacements. In classical plate theory, shear deformation through the thickness is neglected according to Kirchhoff hypothesis. In this thesis however, Mindlin plate theory is used which allows rotations of lines originally perpendicular to the midplane but having no warping. The exclusion of warping is incorrect as shear varies parabolically through the thickness of the plate. The error induced by this inconsistency is reduced to an acceptable level by the introduction of a shear correction factor k . The magnitude of k was calculated by Whitney [15] and the resulting value of $5/6$ is used in the constitutive relations for transverse shear.

From the definition of engineering strain, the relationships for the interlaminar shear strains are

$$\gamma_{yz} = \frac{\partial v}{\partial z} + \frac{\partial w}{\partial y} = \psi_y + w_y \quad (29)$$

$$\gamma_{xz} = \frac{\partial u}{\partial z} + \frac{\partial w}{\partial x} = \psi_x + w_x \quad (30)$$

Substituting Eqs. (29) and (30) into Eq. (15), and introducing the shear correction factor k , the shear stress can be expressed as

$$\begin{Bmatrix} \gamma_{yz} \\ \gamma_{xz} \end{Bmatrix} = k \begin{bmatrix} \bar{Q}_{44} & \bar{Q}_{45} \\ \bar{Q}_{45} & \bar{Q}_{55} \end{bmatrix} \begin{Bmatrix} w_y + \psi_y \\ w_x + \psi_x \end{Bmatrix} \quad (31)$$

The resultant shear forces through the thickness, Q_x and Q_y , are evaluated by integrating the shear stresses in each layer through the laminate thickness. Thus,

$$Q_x = \int_{-h/2}^{h/2} \gamma_{xz} dz = \sum_{k=1}^N \int_{z_{k-1}}^{z_k} \{\gamma_{xz}\}_k dz \quad (32)$$

$$Q_y = \int_{-h/2}^{h/2} \gamma_{yz} dz = \sum_{k=1}^N \int_{z_{k-1}}^{z_k} \{\gamma_{yz}\}_k dz \quad (33)$$

As was done for in-plane forces and moments, the integrations may be simplified by noting that the stiffnesses, \bar{Q}_{ij} , are

constant within the laminae and the shear forces are independent of z . Thus

$$\begin{aligned} Q_y &= k A_{44} A_{45} w_y + \psi_y \\ Q_x &= A_{45} A_{55} w_x + \psi_x \end{aligned} \quad (34)$$

where A_{ij} is defined by Eq. (26)

The equations of motion for the laminated plate may now be derived as all terms appearing in those equations are now defined in terms of the three unknown displacements, $w(x, y, t)$, $\psi_x(x, y, t)$, and $\psi_y(x, y, t)$. A Newtonian approach is used to derive the three governing equations of motion. Figure 3.4 presents the nomenclature for the moment and transverse shear resultants.

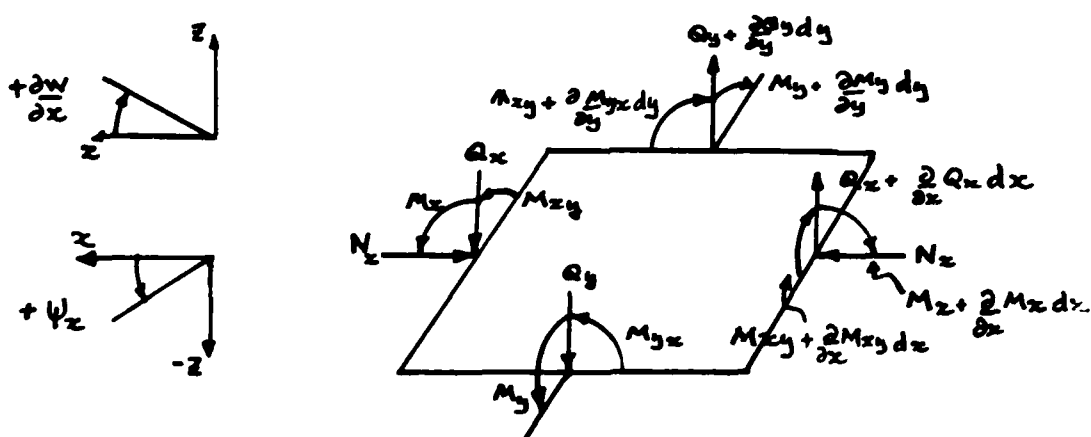


Figure 2.4. Moment and Shear Resultants on Plate

Considering the forces in the z -direction,

$$\sum F_z = \rho h w_{,tt} = Q_x + Q_{x,x} dx - Q_x + Q_{y,y} dy - Q_y + q \quad (35)$$

where $q = N_x w_{xx} + N_y w_{yy}$
 $\rho = \text{plate mass density}$
 $h = \text{plate thickness}$ (36)

Taking moments about the x-axis

$$\begin{aligned} \Sigma M_x = I \psi_{y,tt} &= M_y + M_{y,y} dy - M_y - Q_y dy - Q_{y,y} (dy)^2 \\ &+ M_{xy} + M_{xy,x} dx - M_{xy} \end{aligned} \quad (37)$$

Taking moments about the y-axis

$$\begin{aligned} \Sigma M_y = I \psi_{x,tt} &= M_x + M_{x,x} dx - M_x - M_{yx} + M_{yx} + M_{yx,y} dy \\ &- Q_x dx - Q_{x,x} (dx)^2 \end{aligned} \quad (38)$$

where $I = \int_{-h/2}^{h/2} \rho z^2 dz = \rho h^3 / 12$ (39)

These equations may be simplified if higher order terms are neglected and $dx=dy=1$ is assumed. Substituting in for q , Eqs. (35), (37), and (38) are rewritten in the form

$$Q_{x,x} + Q_{y,y} + N_x w_{xx} + N_y w_{yy} = \rho h w_{tt} \quad (40)$$

$$M_{x,x} + M_{xy,y} - Q_x = I \psi_{y,tt} \quad (41)$$

$$M_{xy,x} + M_{y,y} - Q_y = I \psi_{x,tt} \quad (42)$$

These three equations can now be expressed in terms of the displacements by substituting Eqs. (25) and (34) into the equations of motion. However, before doing so, two restrictions must be applied in order for this problem to be solved using the Levy technique. This thesis considers only symmetric laminates and further, only those which are specially-orthotropic. These restrictions remove all coupling stiffnesses (B_{ij}) and bending-twisting coupling stiffness, D_{16} and D_{26} , reducing Eqs. (25) and (34) to

$$\begin{Bmatrix} M_x \\ M_y \\ M_{xy} \end{Bmatrix} = \begin{bmatrix} D_{11} & D_{12} & 0 \\ D_{12} & D_{22} & 0 \\ 0 & 0 & D_{66} \end{bmatrix} \begin{Bmatrix} \psi_{x,x} \\ \psi_{y,y} \\ \psi_{xy} + \psi_{y,x} \end{Bmatrix} \quad (43)$$

$$\begin{Bmatrix} Q_y \\ Q_x \end{Bmatrix} = k \begin{bmatrix} A_{44} & 0 \\ 0 & A_{55} \end{bmatrix} \begin{Bmatrix} w_{,y} + \psi_y \\ w_{,x} + \psi_x \end{Bmatrix} \quad (44)$$

Assuming the time dependence of the displacements to be harmonic then $e^{i\omega t}$ allows the separation of the time variable out of the equations of motion. Thus, the equations of motion can be written in a form containing only displacements:

$$\begin{aligned} kA_{55} (w_{,xx} + \psi_{x,x}) + kA_{44} (w_{,yy} + \psi_{y,y}) + N_x w_{,xx} + N_y w_{,yy} \\ + \rho h \omega^2 w = 0 \end{aligned} \quad (45)$$

$$D_{11} \psi_{x,xx} + D_{12} \psi_{y,xy} + D_{66} \psi_{x,yy} + D_{66} \psi_{y,xy} - kA_{55} (w_x + \psi_x) \\ + \omega^2 I \psi_x = 0 \quad (46)$$

$$D_{12} \psi_{x,xy} + D_{22} \psi_{y,yy} + D_{66} \psi_{x,xy} + D_{66} \psi_{y,xx} - kA_{44} (w_y + \psi_y) \\ + \omega^2 I \psi_y = 0 \quad (47)$$

where ω is the plate natural frequency

ρ is the plate mass density lb/in^3

These are the three coupled partial differential equations of motion which are solved for the plate displacements with the use of the Levy technique.

LEVY TECHNIQUE

The partial differential equations describing the plate displacement have been formulated and must now be solved. The technique employed in this thesis to solve Eqs (45), (46) and (47) is the Levy technique. This technique is unlike some of the approximate energy techniques (Galerkin, Rayleigh-Ritz, Navier) used previously to study the problem of composite plate stability and vibration. The Levy technique leads to a more exact solution as it removes the errors associated with series representations of the variable. Each displacement term in the equations of motion becomes a single unknown value, as opposed to a series of unknown variables. The mechanics of the Levy technique are presented in the next section, as applied to the specially orthotropic plate, in order to clarify some of the general characteristics of the method presented here.

One of the major restrictions of this method is the requirement that boundaries on two opposite sides of the plate be maintained as simple throughout the analysis so that the description of the plate displacements may have the forms

$$w(x, y, t) = [w(x, y)] e^{i\omega t} = \sum_{n=1}^{\infty} w_n(y) \sin \frac{n\pi x}{a} e^{i\omega t} \quad (48)$$

$$\psi_x(x, y, t) = [\psi_x(x, y)] e^{i\omega t} = \sum_{n=1}^{\infty} \psi_x(y) \cos \frac{n\pi x}{a} e^{i\omega t} \quad (49)$$

$$\psi_y(x, y, t) = [\psi_y(x, y)] e^{i\omega t} = \sum_{n=1}^{\infty} \psi_y(y) \sin \frac{n\pi x}{a} e^{i\omega t} \quad (50)$$

where ω = natural frequency

These forms for the displacement satisfy the mathematical requirements for edges which are simply-supported at $x=0$ and $x=a$ given by Eq. (51) and are used to simplify the equations of motion. Note that the time variable may be factored out of the expressions for displacement. This leaves functions in only x and y to be substituted into the equations of motion.

Simply supported edge at $x=x$ $w(x,y) = \psi_x(x,y) = \psi_y'(x,y) = 0$ (51)

where the prime denotes differentiation w.r.t.y.

Application of Levy Technique to Anisotropic Laminated Plate

Much has been said on the benefits of using the Levy technique to solve the stability and vibration problems for a composite plate. At this point, the actual simplifications of the equations of motion are presented. The resulting equations are then re-written in a form that is useful in solving either the stability or the vibration problem.

In order to use the displacements, as described in Eqs. (48), (49), and (50) in the equations of motion (45-47), the following derivatives are required (note: all Σ are over $n=1$ to ∞ , no time dependence shown).

$$w_{,x} = \sum \frac{n\pi}{a} W \cos \frac{n\pi x}{a}$$

$$w_{,y} = \sum W' \sin \frac{n\pi x}{a}$$

$$w_{,xx} = \sum \left(-\frac{n^2\pi^2}{a^2} \right) W \sin \frac{n\pi x}{a}$$

$$w_{,yy} = \sum W'' \sin \frac{n\pi x}{a}$$

$$\psi_{y,x} = \sum \frac{n\pi}{a} \psi_y \cos \frac{n\pi x}{a}$$

$$\psi_{y,y} = \sum \psi_y' \sin \frac{n\pi x}{a}$$

$$\psi_{y,xx} = \sum \left(-\frac{n^2\pi^2}{a^2} \right) \psi_y \sin \frac{n\pi x}{a}$$

$$\psi_{y,xy} = \sum \frac{n\pi}{a} \psi_y' \cos \frac{n\pi x}{a}$$

$$\psi_{y,yy} = \sum \psi_y'' \sin \frac{n\pi x}{a}$$

$$\begin{aligned}
 \psi_{x,x} &= \sum \frac{-n\pi}{a} \psi_x' \sin \frac{n\pi x}{a} \\
 \psi_{x,y} &= \sum \psi_x' \cos \frac{n\pi x}{a}
 \end{aligned} \tag{52}$$

$$\psi_{x,xx} = \sum \left(\frac{-n^2\pi^2}{a^2} \right) \psi_x \cos \frac{n\pi x}{a}$$

$$\psi_{x,xy} = \sum \frac{-n\pi}{a} \psi_x' \sin \frac{n\pi x}{a}$$

$$\psi_{x,yy} = \sum \psi_x'' \cos \frac{n\pi x}{a}$$

where all primed terms denote differentiation w.r.t.y.

Thus, from Eq. (45),

$$\begin{aligned}
 \sum_{n=1}^{\infty} \left\{ -\frac{n\pi}{a} k A_{55} \psi_x(y) - \frac{n^2\pi^2}{a^2} k A_{55} W(y) + k A_{44} \psi_y'(y) + k A_{44} W''(y) \right. \\
 \left. - \frac{n^2\pi^2}{a^2} N_x W(y) + N_y W''(y) + \rho h \omega^2 W(y) \right\} \sin \frac{n\pi x}{a} = 0 \tag{53}
 \end{aligned}$$

from Eq. (46)

$$\begin{aligned}
 \sum_{n=1}^{\infty} \left\{ -\frac{n^2\pi^2}{a^2} D_{11} \psi_x(y) + \frac{n\pi}{a} D_{12} \psi_y'(y) + D_{66} \psi_x''(y) + \frac{n\pi}{a} D_{66} \psi_y'(y) \right. \\
 \left. - k A_{55} \psi_x(y) - \frac{n\pi}{a} k A_{55} W(y) + \omega^2 I \psi_x(y) \right\} \cos \frac{n\pi x}{a} = 0 \tag{54}
 \end{aligned}$$

from Eq. (47)

$$\begin{aligned}
 \sum_{n=1}^{\infty} \left\{ -\frac{n\pi}{a} D_{12} \psi_x'(y) + D_{22} \psi_y''(y) - \frac{n\pi}{a} D_{66} \psi_x'(y) - \frac{n^2\pi^2}{a^2} D_{66} \psi_y(y) \right. \\
 \left. - k A_{44} \psi_y(y) - k A_{44} W'(y) + \omega^2 I \psi_y(y) \right\} \sin \frac{n\pi x}{a} = 0 \tag{55}
 \end{aligned}$$

Thus, for the equality to hold, the following equations must be satisfied for each n

From Eq. (53)

$$\begin{aligned} \frac{n\pi}{a} kA_{55} \Psi_x(y) - \frac{n^2\pi^2}{a^2} kA_{55} W(y) + kA_{44} \Psi_y'(y) + kA_{44} W''(y) \\ - \frac{n^2\pi^2}{a^2} N_x W(y) + N_y W''(y) + \rho h \omega^2 W(y) = 0 \end{aligned} \quad (56)$$

From Eq. (54)

$$\begin{aligned} \frac{-n^2\pi^2}{a^2} D_{11} \Psi_x(y) + \frac{n\pi}{a} D_{12} \Psi_y'(y) + D_{66} \Psi_x''(y) + \frac{n\pi}{a} D_{66} \Psi_y'(y) \\ - kA_{55} \Psi_x(y) - \frac{n\pi}{a} kA_{55} W(y) + \omega^2 I \Psi_x(y) = 0 \end{aligned} \quad (57)$$

From Eq. (55)

$$\begin{aligned} -\frac{n\pi}{a} D_{12} \Psi_x'(y) + D_{22} \Psi_y''(y) - \frac{n\pi}{a} D_{66} \Psi_x'(y) - \frac{n^2\pi^2}{a^2} D_{66} \Psi_y(y) \\ - kA_{44} \Psi_y(y) - kA_{44} W'(y) + \omega^2 I \Psi_y(y) = 0 \end{aligned} \quad (58)$$

Thus, the application of the Levy technique reduces partial differential equations (in x and y) to ordinary differential equations in y . Eqs. (56), (57), and (58) may now be used to solve the stability or vibration problem for the specially-orthotropic laminate.

Stability Problem

In the solution of the stability problem, basically a static problem, inertia terms will not be retained in the equations of motion. In addition, this thesis will only consider the case of a unaxial compression force. Thus, $N_y = 0$.

To solve the equations of motion, the classical approach of assuming a very general form for the displacements is followed. Hence, the displacements are taken to be

$$\begin{aligned} w(y) &= A^* e^{\theta y} \\ \psi_x(y) &= B^* e^{\theta y} \\ \psi_y(y) &= C^* e^{\theta y} \end{aligned} \tag{59}$$

where A^* , B^* , and C^* are constants to be evaluated.

Further, a notation is adopted which allows the equations to be written in a more compact and manageable form. Using

$$\begin{aligned} D_{12} + D_{66} &= e \\ D_{66} &= f \\ D_{11} &= g \\ D_{22} &= h \\ -N_x &= r \\ kA_{44} &= z \\ kA_{55} &= z \\ \theta &= t \\ m/a &= N \end{aligned} \tag{60}$$

Substituting the assumed forms for the displacements and appropriate derivatives and using the given notation, the equations of motion may be simplified and re-written in matrix form as

$$\{ \bar{0} \} = \begin{bmatrix} N^2 r + t^2 z - N^2 z & -Nz & tz \\ -Nz & ft^2 - gN^2 - z & ent \\ -tz & -ent & ht^2 - fN^2 - z \end{bmatrix} \begin{Bmatrix} A^* \\ B^* \\ C^* \end{Bmatrix} \quad (61)$$

or $[A_{ij}] \begin{Bmatrix} A^* \\ B^* \\ C^* \end{Bmatrix} = \{ \bar{0} \}$

Note: t contains the function ϵ
 r is the buckling force quantity
and n contains the number of modes

The nontrivial solution to this set of coupled ordinary differential equations is found by considering

$$\det [A_{ij}] = 0 \quad (62)$$

At this point, MACSYMA [3] is used to calculate the factored expression for the determinant. The Macsyma package is available on the AFTINET and a description of the commands used to obtain the final form of the expression described by Eq. (62) is presented in Appendix A.

The resulting equation for the determinant of $[A_{ij}]$ is a sixth order equation in the unknown ϵ . It can be written as

$$A_3 \epsilon^6 + A_2 \epsilon^4 + A_1 \epsilon^2 + A_0 = 0 \quad (63)$$

where the coefficients A_i are given in Appendix A.

This can be reduced to a cubic with the substitution of

$$\theta^2 = \varsigma \quad (64)$$

Thus,

$$A_3 \varsigma^3 + A_2 \varsigma^2 + A_1 \varsigma + A_0 = 0 \quad (65)$$

Eq. (65) can be solved directly for three roots following the trigonometric technique presented by Dickson [4]. The roots may be all real numbers or a single real number and two complex conjugates. A development of the problem involving three real roots is presented first, followed by a discussion of the case of two complex conjugate and one real root.

Under the premise of having three real roots to Eq. (65), the assumption is made that two of the real roots are positive and the third, a negative real number. Any changes to this assumption are discussed in the section formulating transcendental equations for the boundary conditions.

With these assumptions, the following nomenclature is utilized

$$\begin{aligned} \varsigma_1 &= \theta_{1,2}^2 = \alpha^2 \\ \varsigma_2 &= \theta_{3,4}^2 = (i\beta)^2 = -\beta^2 \\ \varsigma_3 &= \theta_{5,6}^2 = \gamma^2 \end{aligned} \quad (66)$$

The positive roots for θ are thus assumed to be α and γ . The displacements described in Eq. (59) may now be expressed in an expanded form as

$$\begin{aligned}
 W(y) &= A_1 e^{\alpha y} + A_2 e^{-\alpha y} + A_3 e^{i\beta y} + A_4 e^{-i\beta y} + A_5 e^{\gamma y} + A_6 e^{-\gamma y} \\
 \psi_x(y) &= B_1 e^{\alpha y} + B_2 e^{-\alpha y} + B_3 e^{i\beta y} + B_4 e^{-i\beta y} + B_5 e^{\gamma y} + B_6 e^{-\gamma y} \quad (67) \\
 \psi_y(y) &= C_1 e^{\alpha y} + C_2 e^{-\alpha y} + C_3 e^{i\beta y} + C_4 e^{-i\beta y} + C_5 e^{\gamma y} + C_6 e^{-\gamma y}
 \end{aligned}$$

As presented, Eq. (67) requires the evaluation of 18 separate constants for each set of boundaries in y . Unfortunately, the bc's define only six relationships thereby making it impossible to evaluate any problem using displacements represented in the form of Eq. (67). However, if relationships between A^*/B^* and A^*/C^* are established, the number of constants to be evaluated drops to six and the problem becomes well-posed. Eq. (61) is used, for this problem as it presents the relationships between A^* , B^* , and C^* in the three differential equations of motion. Since these three equations are coupled, the simultaneous solution of any two for B^* and C^* in terms of A^* will automatically satisfy the third.

Solving the second equation from Eq. (61) for C^* in terms of A^* , B^* :

$$\frac{N^2 A^* - (f\theta^2 - z - N^2 g) B^*}{N\theta} = C^* \quad (68)$$

Substituting this value for C^* into the third Eq. from (61) and simplifying for B^*

$$\frac{[(h\theta^2 - z - N^2 f) Nz - Nez\theta^2]}{[(h\theta^2 - z - N^2 f)(f\theta^2 - z - N^2 g) + N^2 e^2 \theta^2]} A^* = B^* \quad (69a)$$

$$\text{or } \Lambda(\theta) A^* = B^* \quad (69b)$$

$$\text{and thus } \frac{Nz - (f\theta^2 - z - N^2 g) \Lambda(\theta)}{Ne\theta} = A^* = C^* \quad (70a)$$

$$\text{or } \tilde{\Lambda}(\theta) A^* = C^* \quad (70b)$$

It must be realized immediately that $\Lambda(\theta)$ and $\tilde{\Lambda}(\theta)$ are row vectors as the value used for θ can have one of three values α , β or γ . The choice of which θ to use in Eq. (69b) and (70b) depends on the argument of the term multiplied by $\Lambda(\theta)$ or $\tilde{\Lambda}(\theta)$ in the expressions for displacements. Thus, $\Lambda(\theta)$ is equal to $(\Lambda(\alpha), \Lambda(\beta), \Lambda(\gamma))^T$. The discussion is not yet complete as a potential problem exists when calculating $\tilde{\Lambda}(\beta)$.

Since

$$i\beta = \theta$$

evaluation of $\tilde{\Lambda}(\beta)$ using Eq. (70a) gives an expression containing an imaginary number in the denominator. An alternate approach may be used to solve for the expressions of $\Lambda(\beta)$ and $\tilde{\Lambda}(\beta)$ that do not contain the imaginary number. For this case

$$w(y) = A^* \sin \beta y \quad \psi_x(y) = B^* \sin \beta y \quad \text{and} \quad \psi_y(y) = C^* \cos \beta y \quad (71)$$

and substitute these values into the equations of motion. Any two of the coupled equations may be solved for the relationships between A^* , B^* and C^* as was done earlier. The calculations lead to the simplified expressions for $\Lambda(\beta)$ and $\tilde{\Lambda}(\beta)$:

$$\frac{(h\beta^2 + N^2 f + z) Nz - Nez\beta^2}{[N^2 e^2 \beta^2 - (h\beta^2 + N^2 f + z)(f\beta^2 + N^2 g + z)]} = \Lambda(\beta) \quad (72)$$

and

$$\frac{Nz + (f\beta^2 + N^2 g + z) \Lambda(\beta)}{Ne\beta} = \tilde{\Lambda}(\beta) \quad (73)$$

The displacements in terms of only six unknown constants, are respectively

$$\begin{aligned} W(y) &= A_1 e^{\alpha y} + A_2 e^{-\alpha y} + A_3 e^{i\beta y} + A_4 e^{-i\beta y} + A_5 e^{\gamma y} + A_6 e^{-\gamma y} \\ \psi_x(y) &= \Lambda(\alpha) (A_1 e^{\alpha y} + A_2 e^{-\alpha y}) + \Lambda(\beta) (A_3 e^{i\beta y} + A_4 e^{-i\beta y}) + \Lambda(\gamma) (A_5 e^{\gamma y} + A_6 e^{-\gamma y}) \\ \psi_y(y) &= \tilde{\Lambda}(\alpha) (A_1 e^{\alpha y} + A_2 e^{-\alpha y}) + \tilde{\Lambda}(\beta) (A_3 e^{i\beta y} + A_4 e^{-i\beta y}) + \tilde{\Lambda}(\gamma) (A_5 e^{\gamma y} + A_6 e^{-\gamma y}) \end{aligned} \quad (74)$$

With the trigonometric and hyperbolic identities of Eq. (75),

$$\begin{aligned} \sinh x &= 1/2 (e^x - e^{-x}) & \sin x &= 1/2i (e^{ix} - e^{-ix}) \\ \cosh x &= 1/2 (e^x + e^{-x}) & \cos x &= 1/2 (e^{ix} + e^{-ix}) \end{aligned} \quad (75)$$

the displacement equations may be written in a more recognizable form. For example, the displacement in the z direction, $W(y)$ is

$$\begin{aligned} W(y) &= \frac{A_1}{2} e^{\alpha y} + \frac{A_1}{2} e^{-\alpha y} + \frac{A_2}{2} e^{-\alpha y} + \frac{A_2}{2} e^{\alpha y} + \frac{A_3}{2} e^{i\beta y} + \frac{A_3}{2} e^{-i\beta y} \\ &\quad + \frac{A_4}{2} e^{-i\beta y} + \frac{A_4}{2} e^{i\beta y} + \frac{A_5}{2} e^{\gamma y} + \frac{A_5}{2} e^{-\gamma y} + \frac{A_6}{2} e^{-\gamma y} + \frac{A_6}{2} e^{\gamma y} \end{aligned}$$

or alternately

$$\begin{aligned} W(y) &= (A_1 + A_2) \frac{1}{2} (e^{\alpha y} + e^{-\alpha y}) + (A_1 - A_2) \frac{1}{2} (e^{\alpha y} - e^{-\alpha y}) + (A_3 + A_4) \frac{1}{2} (e^{i\beta y} + e^{-i\beta y}) \\ &\quad + (A_3 - A_4) \frac{1}{2i} (e^{i\beta y} - e^{-i\beta y}) + (A_5 + A_6) \frac{1}{2} (e^{\gamma y} + e^{-\gamma y}) + (A_5 - A_6) \frac{1}{2} (e^{\gamma y} - e^{-\gamma y}) \end{aligned}$$

applying the identities of Eq. (75), $W(y)$ becomes

$$W(y) = A \sinh \alpha y + B \cosh \alpha y + C \sin \beta y + D \cos \beta y + E \sinh \gamma y + F \cosh \gamma y \quad (76)$$

$$\text{where } A = A_1 - A_2, \quad B = A_1 + A_2, \quad C = (A_3 - A_4)i$$

$$D = A_3 + A_4, \quad E = A_5 - A_6, \quad F = A_5 + A_6$$

Similarly, $\psi_x(y)$ and $\psi_y(y)$ become

$$\begin{aligned} \psi_x(y) = & \Lambda(\alpha)(A \sinh \alpha y + B \cosh \alpha y) + \Lambda(\beta)(C \sin \beta y + D \cos \beta y) \\ & + \Lambda(\gamma)(E \sinh \gamma y + F \cosh \gamma y) \end{aligned} \quad (77)$$

$$\begin{aligned} \psi_y(y) = & \tilde{\Lambda}(\alpha)(A \cosh \alpha y + B \sinh \alpha y) + \tilde{\Lambda}(\beta)(-C \cos \beta y + D \sin \beta y) \\ & + \tilde{\Lambda}(\gamma)(E \cosh \gamma y + F \sinh \gamma y) \end{aligned} \quad (78)$$

It is important to note that $W(y)$ and $\psi_x(y)$ are even functions and $\psi_y(y)$ odd. This is dictated by the number of derivatives of each expression defined in the equations of motion. Eqs. (76), (77), and (78) represent forms for the displacements which may be evaluated for specific boundary conditions in y . Eqs. (76), (77), and (78) thus represent forms for the displacements which may be evaluated for specific boundary conditions in y . These forms have been derived under the premise that all three roots of Eq. (65) are real numbers.

For the case where the roots of Eq. (65) are complex conjugates and a single real number, the development of corresponding expressions for the displacements is not straight forward. The problem lies in deriving the proportionality functions relating A^*/B^* and A^*/C^* . Without these functions,

the number of unknown constants which must be evaluated at each boundary condition is eighteen and the problem is not solvable. Thus, the author has recognized the possibility that specific roots may be missed under the assumption that all roots to Eq. (65) are real numbers. The overall results when plotted however, will indicate trends for a number of different values for a parametric function. The potential of answers not conforming to the associated technique is present but the values will be smeared out in the extrapolation of the function. Thus, the overall trend is extended to any area of difficulty and yields results which are within tolerance of any obtained by trying to reformulate the problem and then solving for the appropriate functional forms of the displacements when only one real root exists. The physical nature of the buckling or vibration phenomena studied in this thesis indicates a lack of irregularities in the solution and thus substantiates this approach to dealing with complex conjugate roots to Eq. (65). The transcendental equations for each of the boundary conditions studied are presented following the development of corresponding forms of the displacements for the vibration problem.

Vibration Problem

For the solution of the vibration problem, the procedures followed will parallel exactly that presented earlier in the stability analysis. Inertia terms, translational and rotary, will be retained in the equations of motion. The in-plane load N_x will of course be excluded from the derivation since the lowest natural frequency will be affected by its presence in the equations of motion.

The forms chosen for the displacements, given by Eq. (59) are used to solve the equations of motion. Additional notation is introduced, to supplement that presented in Eq. (60), representing the inertia terms

$$\omega^2 I = x$$

(79)

$$\rho h \omega^2 = y$$

Using previously defined notation and Eq. (79), the equations of motion in matrix form for the vibration problem are

$$\{\bar{0}\} = \begin{bmatrix} y + t^2 z - N^2 z & -Nz & tz \\ -Nz & x + ft^2 - gN^2 - z & eNt \\ -tz & -eNt & x + ht^2 - fN^2 - z \end{bmatrix} \begin{Bmatrix} A^* \\ B^* \\ C^* \end{Bmatrix} \quad (80)$$

or $[A_{ij}] \begin{Bmatrix} A^* \\ B^* \\ C^* \end{Bmatrix} = \{\bar{0}\}$

Considering the nontrivial solution to this set of equations, the expression for $\det[A_{ij}]$ is presented in Appendix B. The resulting sixth order equation in θ may be reduced to a third order equation by the substitution defined in Eq. (64)

The cubic in ζ is

$$B_3\zeta^3 + B_2\zeta^2 + B_1\zeta + B_0 = 0 \quad (81)$$

where the coefficients B_i are given in Appendix B.

The roots of Eq. (81) can be expressed in terms of α , β , and γ and the expanded expressions for the displacements are identical to those described in Eq. (67). Once again, a relationship is sought between the constants A^* , B^* and C^* and the expressions corresponding to $\Lambda(\theta)$ and $\tilde{\Lambda}(\theta)$ for the vibration problem are given by

$$\frac{[h\theta^2 - z - N^2 f + x)Nz - Nez\theta^2]}{[(h\theta^2 - z - N^2 f + x)(f\theta^2 - z - N^2 g + x) + N^2 e^2 \theta^2]} A^* = B^* \quad (82a)$$

$$\text{or } \Omega(\theta)A^* = B^* \quad (82b)$$

$$\text{and } \frac{Nz - (f\theta^2 - z - N^2 g + x)\Omega(\theta)}{Ne\theta} A^* = C^* \quad (83a)$$

$$\text{or } \tilde{\Omega}(\theta)A^* = C^* \quad (83b)$$

As before, the alternate forms required for the case of $\theta=i\beta$ are given by

$$\frac{(h\beta^2 + N^2 f + z - x) Nz - Nez\beta^2}{[N^2 e^2 \beta^2 - (h\beta^2 + N^2 f + z - x) (f\beta^2 + N^2 g + z - x)]} = \Omega(\beta) \quad (84)$$

and

$$\frac{Nz + (N^2 g + f\beta^2 + z - x) \Omega(\beta)}{Ne\beta} = \tilde{\Omega}(\beta) \quad (85)$$

The final forms for the displacement, shown in Eqs. (76), (77), and (78), remain basically the same the only difference being the multiplication factors. Thus,

$$w(y) = A \sinh \alpha y + B \cosh \alpha y + C \sin \beta y + D \cos \beta y + E \sinh \gamma y + F \cosh \gamma y \quad (86)$$

$$\begin{aligned} \psi_x(y) &= \Omega(\alpha) (A \sinh \alpha y + B \cosh \alpha y) + \Omega(\beta) (C \sin \beta y + D \cos \beta y) \\ &+ \Omega(\gamma) (E \sinh \gamma y + F \cosh \gamma y) \end{aligned} \quad (87)$$

$$\begin{aligned} \psi_y(y) &= \tilde{\Omega}(\alpha) (A \cosh \alpha y + B \sinh \alpha y) + \tilde{\Omega}(\beta) (-C \cos \beta y + D \sin \beta y) \\ &+ \tilde{\Omega}(\gamma) (E \cosh \gamma y + F \sinh \gamma y) \end{aligned} \quad (88)$$

These equations are used in establishing the transcendental equations for the natural frequencies.

Formulation of Transcendental Equations

As the equations for the displacements are similar for the stability and vibration problems, transcendental equations for each boundary condition in y are developed only for the stability case. Corresponding equations for the vibration analysis follow directly by substituting $\Omega(\theta)$ for $\Lambda(\theta)$ and $\tilde{\Omega}(\theta)$ for $\tilde{\Lambda}(\theta)$. Each boundary condition in y is considered independently and the simplified equations for the displacements, in terms of only three constants, are presented in matrix form. The transcendental equation for each case is obtained by taking the determinant of the three by three matrix.

Simple-Simple Boundaries

For the case of simple-simple boundary conditions in y , the following physical and resulting mathematical conditions are used to define the constants in the displacement expressions.

Physically at $y=\tilde{y}$ $w(x, \tilde{y}) = \psi_x(x, \tilde{y}) = M_x(x, \tilde{y}) = 0$

Mathematically $w(\tilde{y}) = \psi_x(\tilde{y}) = \psi_y(\tilde{y}) = 0$ (89)

Note: \tilde{y} represents a general y position of the boundary

If Eq. (89) is used to solve for the constants in the displacement equations, the following results are obtained:

$$A=B=D=E=F=0$$

and for a non-trivial solution

$$\sin \beta b = 0$$

$$\text{or} \quad \beta b = n\pi$$

Thus, for the simple-simple boundaries in y there two positive, one negative real roots to Eq. (65), the relationship that is programmed and solved for N_x is straight forward:

$$\det = \beta - \pi/b \quad (90)$$

$$\text{and} \quad n = 1$$

If three positive real roots exist, the expression that must be solved at $y=b$ becomes

$$\begin{aligned} W(b) &= 0 = A \sinh \alpha b + C \sinh \beta b + E \sinh \gamma b \\ \psi_x(b) &= 0 = A v_1 \sinh \alpha b + C v_2 \sinh \beta b + E v_3 \sinh \gamma b \\ \psi_y'(b) &= 0 = A \alpha v_4 \sinh \alpha b + C \beta v_5 \sinh \beta b + E \gamma v_6 \sinh \gamma b \end{aligned} \quad (91)$$

Thus, the $\sin \beta y / \cos \beta y$ terms in the displacements are replaced by $\sinh \beta y / \cosh \beta y$ if the third root is positive real.

The matrix expression for Eq. (91) is

$$[a_{ij}] \begin{Bmatrix} A \\ C \\ E \end{Bmatrix} = \{0\} \quad (92)$$

where

$$\begin{array}{lll} a_{11} = \sinh \alpha b & a_{12} = \sinh \beta b & a_{13} = \sinh \gamma b \\ a_{21} = v_1 \sinh \alpha b & a_{22} = v_2 \sinh \beta b & a_{23} = v_3 \sinh \gamma b \\ a_{31} = v_4 \alpha \sinh \alpha b & a_{32} = v_5 \beta \sinh \beta b & a_{33} = v_6 \gamma \sinh \gamma b \end{array}$$

where

$$\begin{array}{lll} v_1 = \Lambda(\alpha) & v_2 = \Lambda(\beta) & v_3 = \Lambda(\gamma) \\ v_4 = \tilde{\Lambda}(\alpha) & v_5 = \tilde{\Lambda}(\beta) & v_6 = \tilde{\Lambda}(\gamma) \end{array} \quad (93)$$

Clamped-Clamped Boundaries

The following physical and mathematical conditions define a clamped boundary at $y=\tilde{y}$

$$\text{Physically } w(x, \tilde{y}) = \psi_x(x, \tilde{y}) = \psi_y(x, \tilde{y}) = 0$$

$$\text{Mathematically } w(\tilde{y}) = \psi_x(\tilde{y}) = \psi_y(\tilde{y}) = 0 \quad (94)$$

Thus, at $y=0$, the displacements become

$$w(0) = 0 = B + D + F$$

$$\psi_x(0) = 0 = Bv_1 + Dv_2 + Fv_3 \quad (95)$$

$$\psi_y(0) = 0 = Av_4 - Cv_5 + Ev_6$$

Solving Eq. (95) in terms of the three constants yields

$$D = B \frac{v_1 - v_3}{v_3 - v_2} = Bv_7 \quad (96)$$

$$F = B \frac{v_2 - v_1}{v_3 - v_2} = Bv_8 \quad (97)$$

$$E = C \frac{v_5}{v_6} - A \frac{v_4}{v_6} \quad (98)$$

Using the relationships described by Eq. (96), (97), and (98) the BC's equations can be determined as a function of A, B, and C at $y=b$. This yields the following matrix equation:

$$[a_{ij}] \begin{Bmatrix} A \\ B \\ C \end{Bmatrix} = \begin{Bmatrix} \bar{0} \end{Bmatrix} \quad (99)$$

where

$$a_{11} = \frac{\sinh \alpha b - v_4 \sinh \gamma b}{v_6}$$

$$a_{12} = \cosh \alpha b + v_7 \cos \beta b + v_8 \cosh \gamma b$$

$$a_{13} = \sin \beta b + v_5 \sinh \gamma b$$

$$a_{21} = \frac{v_1 \sinh \alpha b - v_1 v_4 \sinh \gamma b}{v_6}$$

$$a_{22} = v_1 \cosh \alpha b + v_2 v_7 \cos \beta b + v_3 v_8 \cosh \gamma b$$

$$a_{23} = v_2 \sin \beta b + v_3 v_5 \sinh \gamma b$$

$$a_{31} = v_4 \cosh \alpha b - v_4 \cosh \gamma b$$

$$a_{32} = v_4 \sinh \alpha b + v_5 v_7 \sin \beta b + v_6 v_8 \sinh \gamma b$$

$$a_{33} = -v_5 \cos \beta b + v_5 \cosh \gamma b$$

where α , β and γ are variables and v_i are functions of these variables

Simple-Clamped Boundaries

The mathematical conditions describing the simple and clamped boundaries are given by Eqs. (89) and (94). Considering a simple boundary at $y=0$ leads to

$$W(0) = 0 = B + D + F$$

$$\Psi_x(0) = 0 = Bv_1 + Dv_2 + Fv_3 \quad (100)$$

$$\Psi_y'(0) = Bv_4 + Dv_5 + Fv_6$$

$$\text{or} \quad B = D = F = 0 \quad (101)$$

A clamped boundary at $y=b$ gives

$$W(b) = 0 = Asinh\alpha b + Csinf\beta b + Esinh\gamma b$$

$$\Psi_x(b) = 0 = Av_1 sinh\alpha b + Cv_2 sin\beta b + Ev_3 sinh\gamma b \quad (102)$$

$$\Psi_y'(b) = 0 = Av_4 cosh\alpha b - Cv_5 cos\beta b + Ev_6 cosh\gamma b$$

Eq. (102) in matrix form becomes

$$[a_{ij}] \begin{Bmatrix} A \\ C \\ E \end{Bmatrix} = \{0\} \quad (103)$$

where

$$a_{11} = sinh\alpha b \quad a_{12} = sin\beta b \quad a_{13} = sinh\gamma b$$

$$a_{21} = v_1 sinh\alpha b \quad a_{22} = v_2 sin\beta b \quad a_{23} = v_3 sinh\gamma b$$

$$a_{31} = v_4 cosh\alpha b \quad a_{32} = -v_5 cos\beta b \quad a_{33} = v_6 cosh\gamma b$$

Simple-Free Boundaries

A simple boundary at $y = 0$ leads to the relationships between constants given by Eq. (101). A free boundary, at $y = b$, has the following physical and mathematical conditions

$$\text{Physically} \quad M_y = M_{xy} = Q_y = 0$$

$$\text{Mathematically} \quad M_y = -ND_{12}\Psi_x(b) + D_{22}\Psi_y'(b) = 0 \quad (104)$$

$$M_{xy} = \Psi_x'(b) + N\Psi_y(b) = 0$$

$$Q_y = W'(b) + \Psi_y(b) = 0$$

Expanding Eq. (104) and placing in matrix form gives

$$[a_{ij}] \begin{Bmatrix} A \\ C \\ E \end{Bmatrix} = \{ \bar{0} \} \quad (105)$$

where

$$a_{11} = (D_{22}^\alpha v_4 - ND_{12}v_1) \sinh \alpha b$$

$$a_{12} = (D_{22}^\beta v_5 - ND_{12}v_2) \sin \beta b$$

$$a_{13} = (D_{22}^\gamma v_6 - ND_{12}v_3) \sinh \gamma b$$

$$a_{21} = (\alpha v_1 + Nv_4) \cosh \alpha b$$

$$a_{22} = (\beta v_2 - Nv_5) \cos \beta b$$

$$a_{23} = (\gamma v_3 + Nv_6) \cosh \gamma b$$

$$a_{31} = (\alpha + v_4) \cosh \alpha b$$

$$a_{32} = (\beta - v_5) \cos \beta b$$

$$a_{33} = (\gamma + v_6) \cosh \gamma b$$

Clamped-Free Boundaries

A clamped boundary at $y=0$ gives the relationships described by Eqs. (96), (97), and (98)

$$D = Bv_7 \quad (96)$$

$$F = Bv_8 \quad (97)$$

$$E = Cv_5/v_6 - Av_4/v_6 \quad (98)$$

Substituting these relationships into the expanded form of Eq.

(104) and rewriting in matrix form gives

$$[a_{ij}] \begin{Bmatrix} A \\ B \\ C \end{Bmatrix} = \{ \bar{0} \} \quad (106)$$

where

$$a_{11} = \frac{(-ND_{12}v_1 + D_{22}^\alpha v_4) \sinh \alpha b + (v_3 v_4 ND_{12} - D_{22}^\gamma v_4) \sinh \gamma b}{v_6}$$

$$a_{12} = (-ND_{12}v_1 + D_{22}\alpha v_4) \cosh \alpha b + (-ND_{12}v_2 + D_{22}\beta v_5) v_7 \cosh \beta b \\ + (-ND_{12}v_3 + D_{22}\gamma v_6) v_8 \cosh \gamma b$$

$$a_{13} = \frac{(-ND_{12}v_2 + D_{22}\beta v_5) \sin \beta b + (-ND_{12}v_3 v_5 + D_{22}\gamma v_5) \sinh \gamma b}{v_6}$$

$$a_{21} = \frac{(\alpha v_1 + Nv_4) \cosh \alpha b - (\gamma v_3 v_4 + v_4) \cosh \gamma b}{v_6}$$

$$a_{22} = \frac{(\alpha v_1 + Nv_4) \sinh \alpha b - (\beta v_2 + Nv_5) v_7 \sin \beta b + (\gamma v_3 + Nv_6) v_8 \sinh \gamma b}{v_6}$$

$$a_{23} = \frac{(\beta v_2 - Nv_5) \cos \beta b + (\gamma v_3 v_5 + Nv_5) \cosh \gamma b}{v_6}$$

$$a_{31} = \frac{(\alpha + v_4) \cosh \alpha b - (\gamma v_4 + v_4) \cosh \gamma b}{v_6}$$

$$a_{32} = \frac{(\alpha + v_4) \sinh \alpha b + (-\beta + v_5) v_7 \sin \beta b + (\gamma + v_6) v_8 \sinh \gamma b}{v_6}$$

$$a_{33} = \frac{(\beta - v_5) \cos \beta b + (\gamma v_5 + v_5) \cosh \gamma b}{v_6}$$

Free-Free Boundaries

A free boundary, as defined mathematically by Eq. (104), gives for $y=0$

$$M_y = -ND_{12}[v_1B + v_2D + v_3F] + D_{22}[v_4\alpha B + v_5\beta D + v_6\gamma F] = 0 \quad (107)$$

$$M_{xy} = v_1A + v_2C + v_3E + N[v_4A - v_5C + v_6E] = 0 \quad (108)$$

$$Q_y = v_4A - v_5C + v_6E + A\alpha + C\beta + E\gamma = 0 \quad (109)$$

from Eq. (107), E can be written in terms of A and C as

$$\frac{-(Nv_4 + v_1)}{(v_3 + Nv_6)} A + \frac{(Nv_5 - v_2)}{(v_3 + Nv_6)} C = E \quad (110)$$

or

$$v_7A + v_8C = E \quad (111)$$

With this relationship and Eq. (109), a relationship between A and C is developed

$$\frac{(v_4 + \alpha) - (v_6 + \gamma)(Nv_4 + v_1)}{(Nv_6 + v_3)} A + \frac{(\beta - v_5) + (v_6 + \gamma)(Nv_5 - v_2)}{(Nv_6 + v_3)} C = 0 \quad (112)$$

or

$$v_9A + v_{10}C = 0 \quad (113)$$

thus

$$C = \frac{-v_9A}{v_{10}} = \frac{v_{11}A}{v_{10}} \quad (114)$$

and it follows from Eq. (111) that

$$(v_7 + v_8v_{11}) A = E \quad (115)$$

or

$$v_{12} A = E$$

from Eq. (107)

$$\frac{(D_{22}\alpha v_4 - ND_{12}v_1)}{(ND_{12}v_3 - D_{22}\gamma v_6)} B + \frac{(D_{22}\beta v_5 - ND_{12}v_2)}{(ND_{12}v_3 - D_{22}\gamma v_6)} D = F \quad (116)$$

or

$$v_{13}B + v_{14}D = F \quad (117)$$

Introducing the relationships between the constants to the relationships for a free boundary at $y=b$ and expressing in matrix form leads to

$$[a_{ij}] \begin{Bmatrix} A \\ B \\ D \end{Bmatrix} = \begin{Bmatrix} 0 \end{Bmatrix} \quad (118)$$

where

$$a_{11} = (-ND_{12}v_1 + D_{22}v_4^\alpha) \sinh \alpha b + (-ND_{12}v_2 v_{11} + D_{22}v_5 v_{11}^\beta) \sinh \beta b + (-ND_{12}v_3 v_{12} + D_{22}v_6 v_{12}^\gamma) \sinh \gamma b$$

$$a_{12} = (-ND_{12}v_1 + D_{22}v_4^\alpha) \cosh \alpha b + (-ND_{12}v_3 v_{13} + D_{22}v_6 v_{13}^\gamma) \cosh \gamma b$$

$$a_{13} = (-ND_{12}v_2 + D_{22}v_5^\beta) \cos \beta b + (-ND_{12}v_3 v_{14} + D_{22}v_6 v_{14}^\gamma) \cosh \gamma b$$

$$a_{21} = (v_1^\alpha + Nv_4) \cosh \alpha b + (v_2 v_{11}^\beta - Nv_5 v_{11}) \cos \beta b + (v_3 v_{12}^\gamma + Nv_6 v_{12}) \cosh \gamma b$$

$$a_{22} = (v_1^\alpha + Nv_4) \sinh \alpha b + (v_3 v_{13}^\gamma + Nv_6 v_{13}) \sinh \gamma b$$

$$a_{23} = (-v_2^\beta + Nv_5) \sin \beta b + (v_3 v_{14}^\gamma + Nv_6 v_{14}) \sinh \gamma b$$

$$a_{31} = (v_4^\alpha + \alpha) \cosh \alpha b + (-v_5 v_{11} + \beta v_{11}) \cosh \beta b + (v_6 v_{12} + \gamma v_{12}) \cosh \gamma b$$

$$a_{32} = (v_4^\alpha + \alpha) \sinh \alpha b + (v_6 v_{13} + \gamma v_{13}) \sinh \gamma b$$

$$a_{33} = (v_5^\beta - \beta) \sin \beta b + (v_6 v_{14} + \gamma v_{14}) \sinh \gamma b$$

III. Discussion and Results

This chapter presents a brief introduction of the two computer programs written to solve the transcendental equations, generated earlier, for either the stability or vibration problem of a laminated plate. Discussions follow on the physical properties of the plate as well as the analysis performed using the plate.

Computer Programs

One existing computer program is modified and one program is written to solve the respective stability/vibration problem of a rectangular plate with the six different boundary conditions already discussed. The first program is a modification of a program written by Bowlus [2] which calculates the nondimensional bending and extensional stiffnesses for a symmetric laminate. The second program formulates the boundary value problem for a particular boundary condition in y in the form $[a_{ij}]\{c\} = \{0\}$ where $[a_{ij}]$ is the 3×3 matrix containing the eigenvalue and c is a column vector of displacement constants. The program solves the transcendental equation given by $\det [a_{ij}]$ for the value of N_x or ω . Appendix D gives a more detailed description of the second program.

Analysis Performed

Two main areas are analyzed in this thesis, using the data generated by the second program. First, the ability of the Levy technique to effectively solve the various vibration and stability problems formulated earlier. Second, the importance of shear deformation (and for the vibration problem rotary inertia) in a mathematical model of a laminated plate.

The application of the Levy method is validated for the vibration problem by comparing results to those calculated by Bowlus [2]. The boundary conditions used in this comparison will be simple-simple in the y-direction. Due to the similarities in the formulation of the vibration and stability problems, such a comparison will also validate the stability portion of the program. The author could not find other published works for plates with similar geometries/material properties and/or ply lay-ups and different boundary conditions with which to further evaluate the second program. General trends and expectations for specific boundary conditions are available however, and are used in the later discussions of the results.

The impact or importance of shear deformation is evaluated by altering the length to thickness ratio of the plate. For the vibration problem, rotary inertia is introduced into the model and a second set of calculations performed. For three of the boundaries, notably simple-simple, simple-clamped and simple-free, a square plate is used in the calculations. For the other three boundary conditions in y, the formulation of the transcendental equations forces the use of rectangular plates with aspect ratios of two or greater due to computational limitations. The analysis follows a presentation

of the material properties of the laminated plates used in this analytical study.

Laminated Composite Plate Properties

The plate studied in this thesis is constructed of a graphite-epoxy (AS/3501) material and has the following material properties

$$\begin{aligned} E_1 &= 21.0E+06 \text{ psi} \\ E_2 &= 1.40E+06 \text{ psi} \\ G_{12} &= 0.6E+06 \text{ psi} \\ \nu_{12} &= 0.3 \\ \rho &= 0.055 \text{ lb/in}^3 \end{aligned} \tag{119}$$

The plate has a ply-layup of $[0, 90]_m$. For the comparison with Bowlus, m equals 100 indicating a total laminate thickness of one inch if each lamina is assumed to be 0.005 inch thick. A plate with m equal to 200 is used for all other calculations. Tables 3.1 and 3.2 contain the stiffness values obtained from the first program for the two plates.

Graphite-Epoxy [0/90]_{100s}

One Inch Thick

Parameter	Value
A_{44}	540,000.3125
A_{55}	540,000.3125
D_{11}	1555164.375
D_{12}	35211.2656
D_{22}	322769.875
D_{66}	50000.0

Units for A_{ij} : lb/in

Units for D_{ij} : lb-in

Table 3.1 Stiffness Parameters for a One Inch Thick Plate

Graphite-Epoxy [0/90]_{200s}

Two Inches Thick

Parameter	Value
A_{44}	1,080,000.625
A_{55}	1,080,000.625
D_{11}	12,441,315.0
D_{12}	281,690.125
D_{22}	2,582,159.0
D_{66}	400,000.0

Units for A_{ij} : lb/in

Units for D_{ij} : lb-in

Table 3.2 Stiffness Parameters for a Two Inch Thick Plate

Characteristics of Levy Technique

In most of the previous studies of laminated plate behavior, proof of convergence of the solutions must be presented. With the Levy technique, the values of N_x or ω are calculated using a closed form algorithm. The only factor that must be ensured is that the value computed is indeed the lowest value for N_x or ω . This is done by repeating the computations for increasing values of n , the bending mode number, until the user is satisfied that the results are continuously increasing. The lowest eigenvalue, regardless of n , is the sought after solution. In most cases, n need not be increased past three to determine the trend of the output.

In order for the program, which is used to evaluate the transcendental equation, to have some credibility, results must be compared with previously published work. As was stated earlier, apart from work by Bowlus, published work on the buckling or vibration of [0/90]_{ms} composite materials was not abundant. Leissa [27,28] and Brunelle [1] have results which can be used to validate trends, but only Bowlus has numerical values which can be used in a direct comparison. Thus, from reference [2] for a plate simply supported on all sides, the following comparison can be made for the first natural frequency.

S (a/h)	Galerkin Method with SD and RI	Levy Method with SD and RI	% Difference
17.5	3754.98	3762.44	0.20
20.0	2899.69	2913.32	0.47
22.5	2310.70	2320.17	0.41
27.5	1559.94	1568.82	0.57
30.0	1321.80	1322.56	0.06
35.0	975.16	976.10	0.10
40.0	752.80	749.47	0.44

Table 3.3 Comparison of Galerkin and Levy Techniques for a Plate Simply-Supported On All Four Edges. Plate Thickness is One Inch.

The values in Table 3.3 show good agreement between the closed form solution and one obtained using the Galerkin technique with the double series containing six terms each.

To further validate the second program, a comparison is presented of the results computed for the simple-clamped boundary in y and the classical solution obtained for the specially orthotropic plate using an equation from Whitney [8]. For a plate with no shear deformation or rotary inertia, the natural frequency can be computed from

$$\omega = \frac{1}{a^2 \sqrt{\rho}} [D_{11} \alpha_1^4 + 2(D_{12} + 2D_{66})R^2 \alpha_2^2 + D_{22} R^4 \alpha_3^4]^{1/2} \quad (120)$$

where

$$R = a/b$$

$$\alpha_1 = (m+.25)\pi$$

$$\alpha_2 = n^2 \pi^2 \alpha_1 (\alpha_1 - 1) \quad (121)$$

$$\alpha_3 = n\pi$$

$$a = 80 \text{ in}$$

$$\rho = 0.055 \text{ lb/in}^3$$

for all m and n. (for fundamental frequency, m=n=1)

Using the properties for the two inch thick plate given in Table 3.2 and computing the natural frequency for a plate where R=1.0, the following is obtained

$$\omega = 769.574 \text{ Hz} \quad (122)$$

This value represents the classical plate solution and can be compared to the value obtained for the natural frequency, using the Levy technique, given in Table 3.4

S (a/h)	Levy Method SD and RI	Levy Method SD no RI
10.0	4891.466	4917.118
12.5	3282.50	3294.
15.0	2344.26	2350.771
17.5	1753.1	1756.
20.0	1358.306	1360.588
22.5	1082.	1083.
25.0	881.889	882.872
27.5	732.	732.

All frequencies are in Hz

Table 3.4 Natural Frequency of Two Inch Thick Plate
With and Without RI. Simple-Clamped
Boundaries in Y.

Thus, as the plate thickness ratio increases and the effects of shear deformation and rotary inertia become negligible, the results approach the classical solution of 769.574Hz. Classical solutions for other boundary conditions or for the stability problem could not be found in the literature.

Analysis of Shear Deformation and Rotary Inertia

The second main area of investigation in the thesis is the importance of including shear deformation in the plate model for the six different boundary conditions proposed for the plate study. In the case of the vibration analysis, the benefits of further model refinement, due to the addition of rotary inertia, is also investigated. The analysis is accomplished by performing calculation for various plate length to thickness ratios and comparing any trends to behavior predicted using classical plate theory.

The following discussion is separated into two sections; the first considers the buckling problem, the second, the free vibration problem.

Buckling Problem

For each boundary condition, increasing length to thickness ratios and length to width ratios are programmed and solved. Computational limitations play a limiting role as far as how many different length to thickness and a/b ratios may be investigated for the various y directed boundaries. In the subsequent presentation of results for each B.C., the range of S and plate aspect ratio for which useful data is obtained is given. (This gives a good indication of the limitations of the program written for this thesis). For all boundaries however, an increase in the length to thickness ratios indicates a decrease in the effect of shear force variations through the thickness. That is, the approximation that shear reformation effects are negligible is increasingly valid as the plate becomes thinner and physical differences in the z direction become very small. The thinner plates quickly

tend to the classical plate behaviour as S is increased past 40. This trend is apparent on all of the subsequent figures depicting non-dimensionalized buckling load $N_x (-N_x a^2 / \pi^2 / D_{11} D_{22})$ vs length to thickness ratio.

The non-dimensionalizing parameter is chosen as it clearly illustrates the effects of two important variables on the buckling load. The first is the length to width ratio (S) of the plate, the second, the aspect ratio of the plate. The curves asymptotically approach limiting value as S increases and this value can be seen to represent the classical laminated solution. No results are presented for length to thickness ratios under 10 for any of the boundary conditions. It is important to realize that the assumptions of plane stress and no strain in the z direction are less and less valid as S decreases. The errors resulting from the assumptions are no longer negligible at length to thickness ratio less than 10 and any results obtained are invalid. By choosing this non-dimensionalizing parameter, the reader also gains a better appreciation of the dependence of the buckling load on the aspect ratio as the latter is varied from two to four.

For the plate simply-supported on all sides, a square configuration is used in calculating the buckling load. Length to thickness is varied from 10 to 30 and the results are presented in Figure 3.1 for the first bending mode. The curve for the non-dimensionalized buckling load is seen to flatten out for S approaching 32.5. The difference at this point between CPT and shear deformation theory (SDT) is negligible. For a thicker plate however, the difference increases to a maximum of 26.8% for an S of 10.

For the plate which is clamped at $y=0$ and $y=b$, a rectangular plate with aspect ratios (a/b) of two, three and four is used in the analysis. Length to

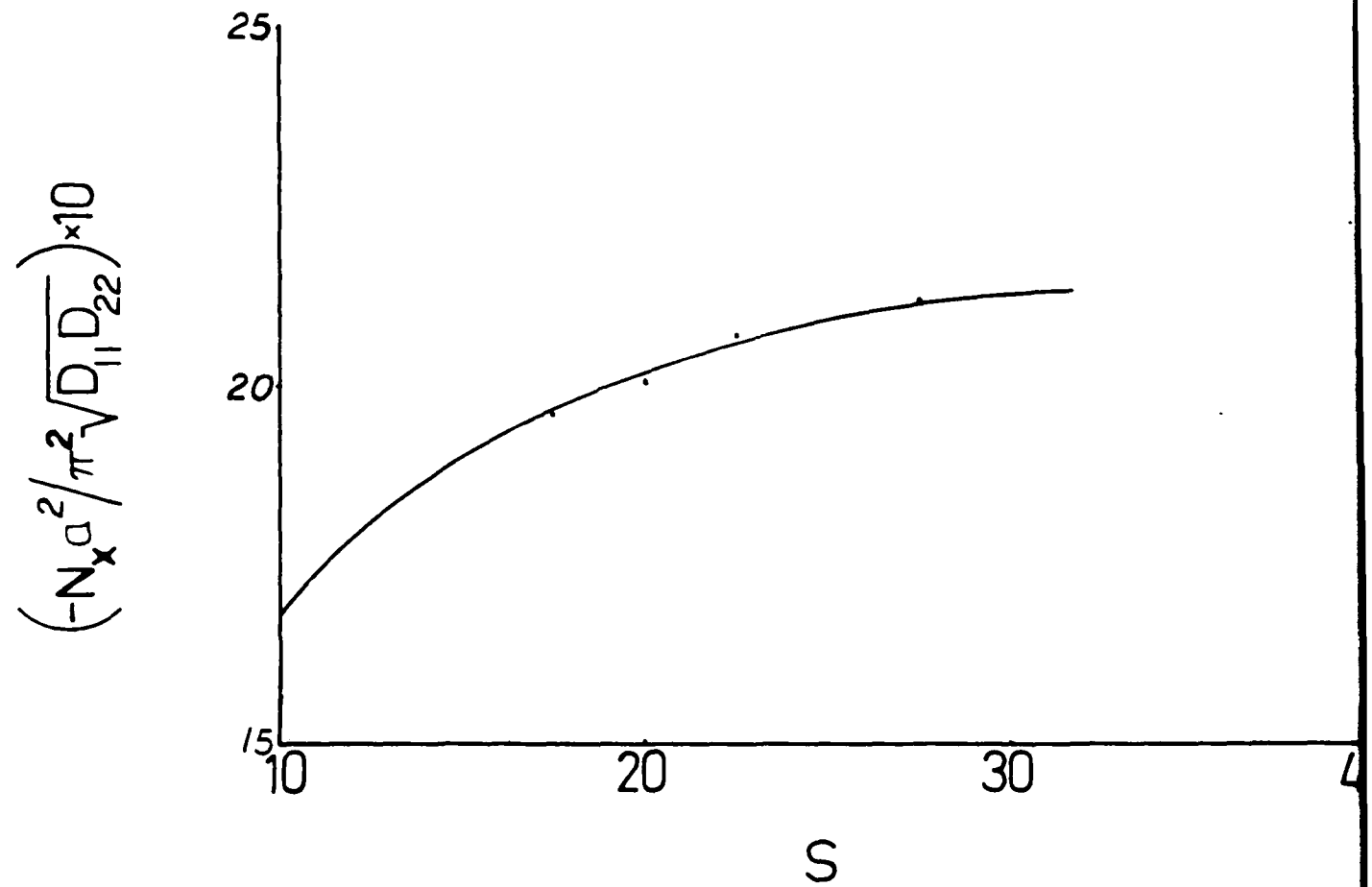


Figure 3.1 Plot of Normalized Buckling Load vs Thickness
Ratio For Simple-Simple Boundaries.

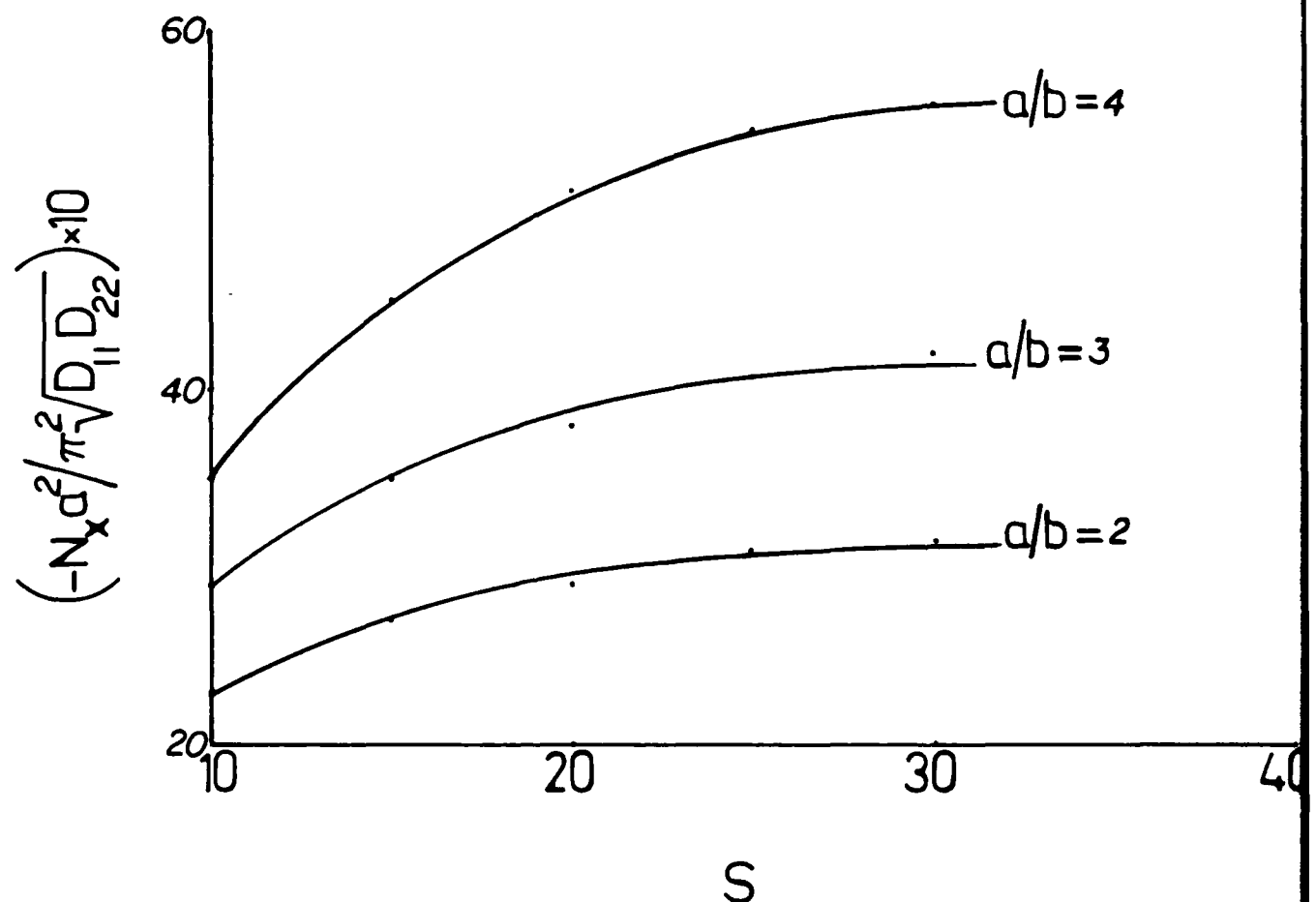


Figure 3.2 Plot of Normalized Buckling Load vs Thickness Ratio for Clamped-Clamped Boundaries.

thickness is varied from 10 to 37.5 for the first plate. The curve of the non-dimensionalized buckling load once again behaves asymptotically as the value of S becomes greater than 30 (See Figure 3.2). For an aspect ratio of two, a maximum difference of 37.14% exists between the SDT value and CPT extrapolated value at S equal to 10. As the aspect ratio increases, the non-dimensionalized buckling load increases. This is misleading as the dimensionalized buckling load, N_x , does in fact decrease, as a/b increases, indicating a decrease in the plates' ability to withstand the uniaxial compressive force. The maximum difference between CPT and SDT, for a/b equal to three, is approximately 36.65%. For a/b of four, S is varied from 20 to 40 with a maximum difference, between the theories, of 36.28% occurring at S equal to 10. CPT solutions for orthotropic plate, presented in reference [28], indicate that a common solution exists for all aspect ratios greater than two. Results shown in Figure 3.2 indicate that plates of different aspect ratios do not have common asymptotic values for S equal to 40. It is apparent that as a/b is increased the difference between asymptotic values does not vanish due to the interaction between boundary and buckling load.

A square plate is used to analyze the simple-clamped boundary conditions in y . The curve in Figure 3.3 is plotted for length to thickness ratios of 10 to 25. Computer limitations prevent larger S values from being used to calculate the buckling load. The maximum difference between SDT and CPT occurs at a length to thickness ratio of 10 and has a magnitude of 29.03%. The extrapolated value for the classically derived buckling load is reached fairly quickly at S equal to 32.5.

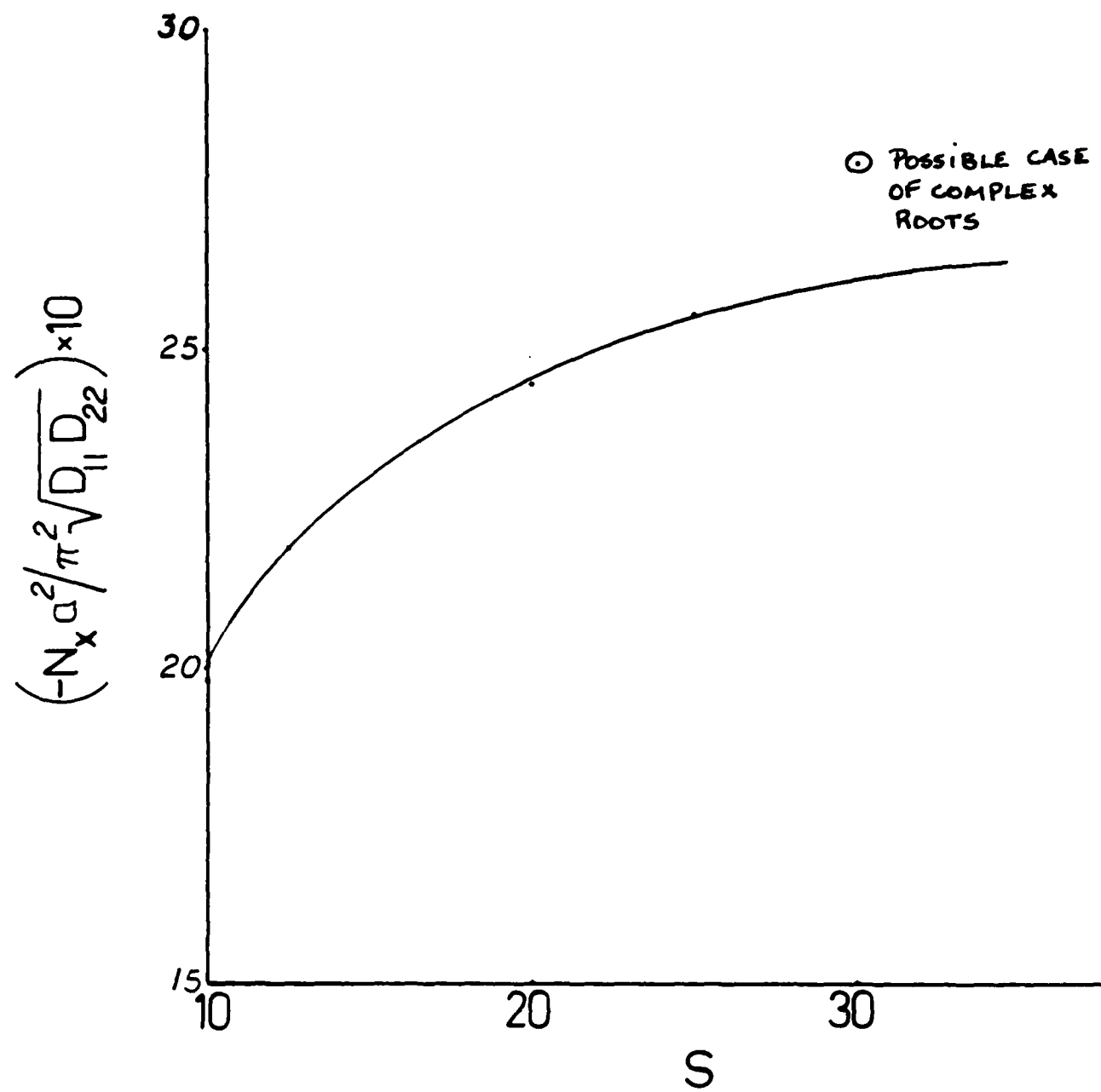


Figure 3.3 Plot of Normalized Buckling Load vs Thickness Ratio For Simple-Clamped Boundaries.

For the simple-free boundaries in y , the behaviour of the square plate is depicted in Figure 3.4. S is varied from 10 to 22.5, the upper limit a function of computer limitations. The results allow the characteristics of this boundary to be studied and a difference, between the two theories, of 23.01% exists at S equal to 10 and decreases as S increases.

The clamped-free y directed boundaries are studied using a rectangular plate with aspect ratios varying from two to four. For a/b of two and three, S is increased from 10 to 30. For a/b of four, S is increased to 40. The three curves are plotted in Figure 3.5. Once again, though the curves show asymptotic behaviour as S is increased, the values at a length to thickness ratio of 40 are different for each plate aspect ratio. This demonstrates the significance of the shear deformation in an accurate model of plate behaviour. Maximum differences between classical theory and shear deformation theory varies from 26.86% to 27.84% as the aspect ratio increases from two to four.

The final results obtained for a buckling problem are presented in Figure 3.6. The free-free boundaries considered are analyzed using a rectangular plate with three different aspect ratios. For a plate aspect ratio of two, the length to thickness ratio is varied from 10 to 40. A difference of 26.92% exists between SDT and CPT at S equal to 10 for this first rectangular plate. For a/b of three, S is also varied from 10 to 40 and the disparity between theories peaks at 23.4% for S equal to 10. The final plate studied, with an aspect ratio of four, has a range for S of 10 to 40. The max divergence between theories, at S equal to 10, is 23.81%.

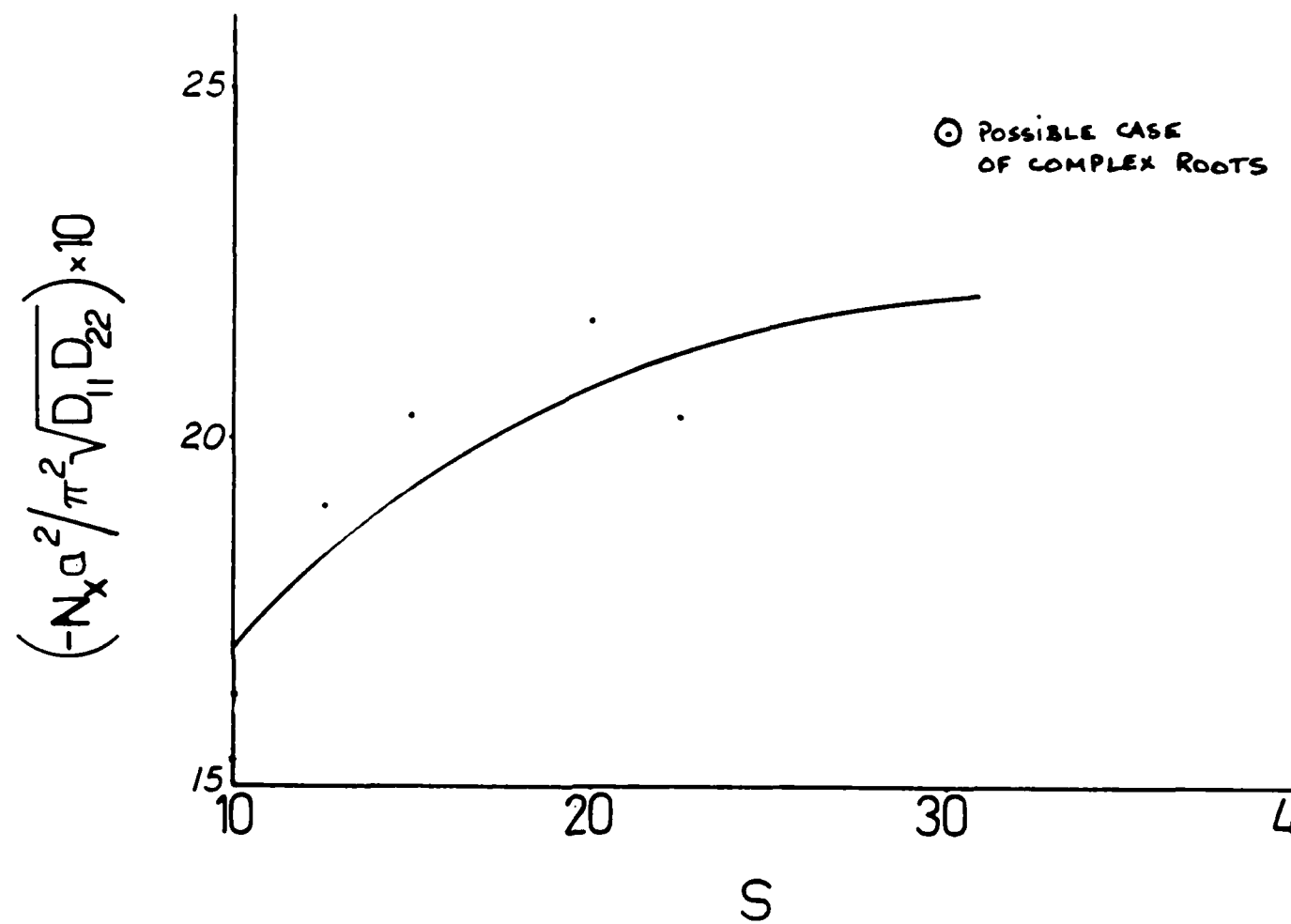


Figure 3.4 Plot of Normalized Buckling Load vs Thickness
Ratio For Simple-Free Boundaries.

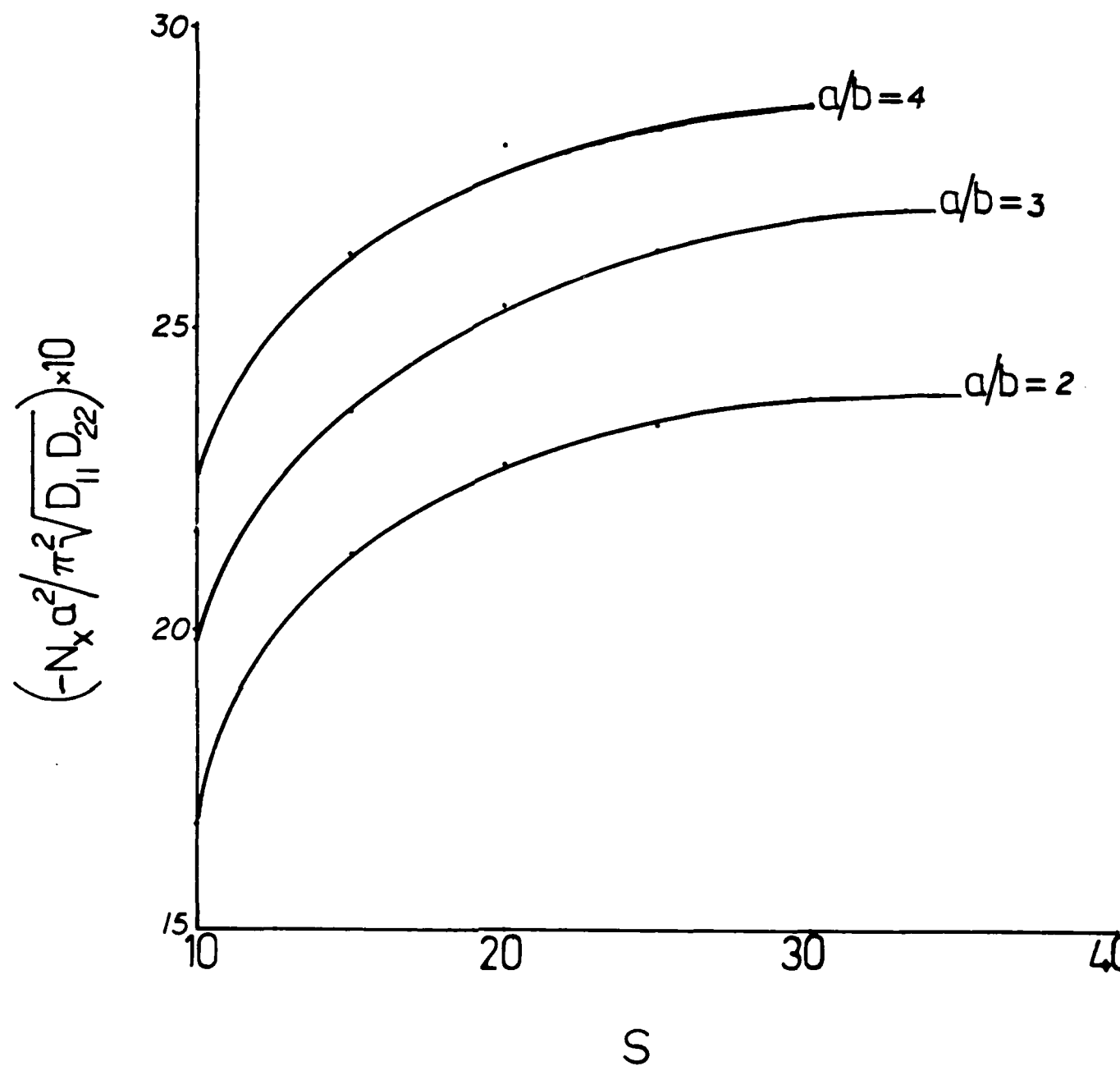


Figure 3.5 Plot of Normalized Buckling Load vs Thickness Ratio For Clamped-Free Boundaries.

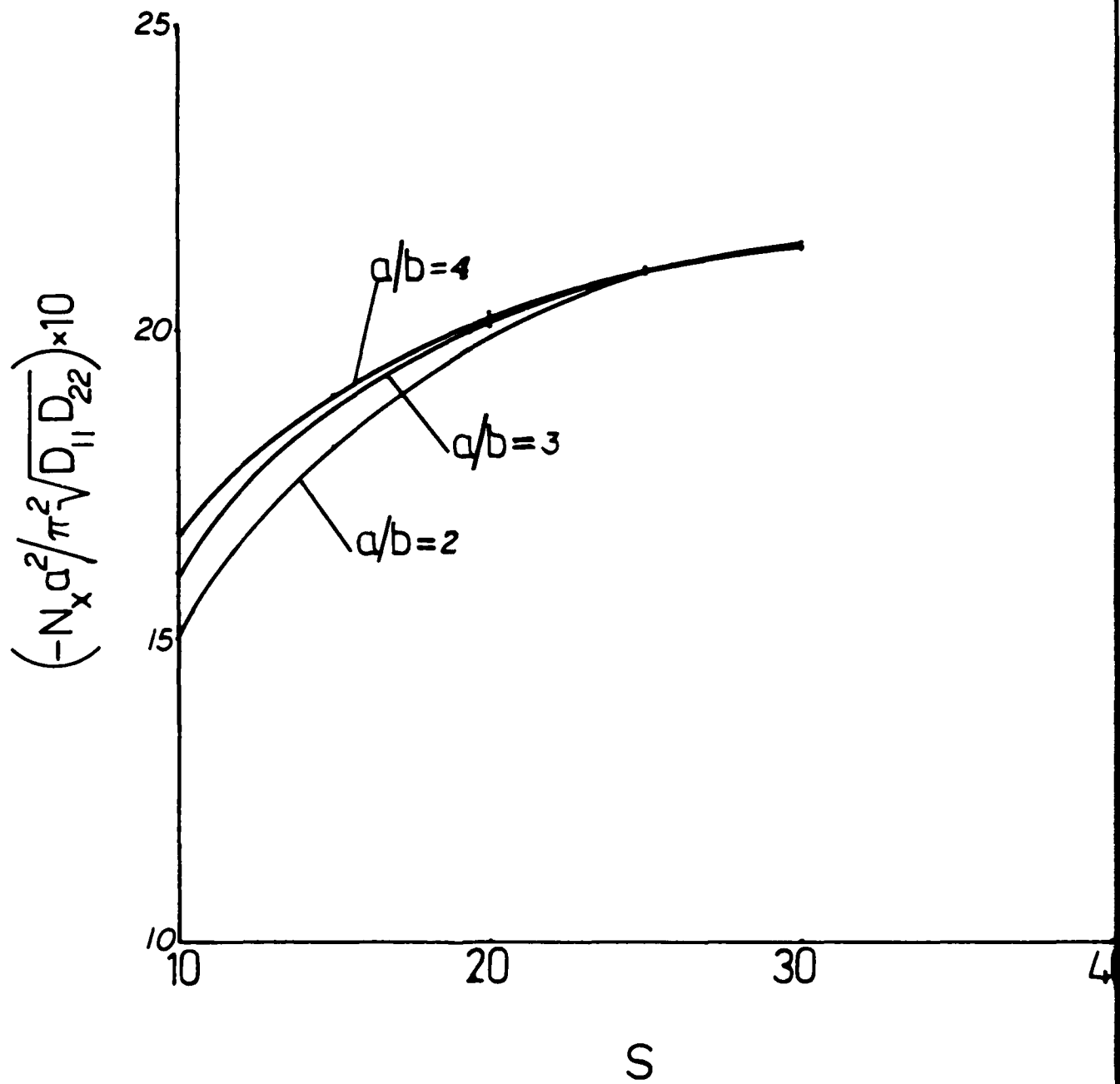


Figure 3.6 Plot of Normalized Buckling Load vs Thickness
Ratio For Free-Free Boundaries.

It is interesting, at this point, to compare some of the results obtained in order to better understand the interaction, if any, between the boundaries in the y direction and shear deformation effects. To do so, plates with similar geometries and different boundary conditions are compared in Table 3.5.

Boundaries in y	Aspect Ratio of Plate	Max Difference between SDT/CPT (%)
SS	1	26.80
SC	1	29.03
SF	1	23.01
CC	2	37.14
CC	3	36.65
CC	4	28.00
CF	2	26.86
CF	3	24.31
CF	4	27.84
FF	2	26.92
FF	3	23.40
FF	4	23.81

Table 3.5 Comparison of Discrepancies Between Shear Deformation Theory and Classical Plate Theory for Stability Problems.

General behaviour characteristics become more apparent from this table. First, the effects of shear deformation are very important regardless of the type of boundaries for the plate. An average difference of 28.50% exists,

regardless of the B.C.'s in y , between the models of plate behaviour for the orientation studied. The effects of shear deformation are somewhat lower for the free-free boundaries than those which have any form of restraint. The free-free boundaries have an average difference of 24.71% compared to 33.18% for the other boundaries in y . This is most likely due to a greater reaction between buckling load and boundaries if the boundaries are prevented from free movement.

Secondly, as the plates get thinner, the shear deformation effects remain important. For the rectangular CF or FF plates under study, the plate behaviour becomes less influenced by the shear deformation as the aspect ratio is increased. In addition, the asymptotic value reached by the plate as it becomes thinner remains different for the range of aspect ratios investigated. Unlike classical theory which predicts a common asymptotic value for all a/b ratios over two (reference [28]), SDT indicates that shear effects, though small, still linger even as S increases to 40. Differences in the asymptotic value do decrease however, as a/b increases for the free boundaries.

Thirdly, the results validate the approach presented in the theory section for dealing with complex conjugate roots to Eq. (65). These roots occur at values of N_x which are lower than for the case of three real roots. Hence, an erroneous root would appear higher than the general trend established with the best-fit curve. For the stability problem, only two such possible cases did occur for all the computations and they are indicated on the respective figures.

Fourthly, the plate aspect ratio is an important parameter to consider in a stability problem if the plate boundaries normal to the applied force provide some restraint. Figure 3.6 clearly shows that free boundaries lead to similar values for critical load regardless of a/b .

Finally, stiffer plate supports result in higher buckling loads. This can be seen by comparing values of N_x calculated for the CC and CF boundaries.

Vibration Problem

In a procedure similar to the one followed for the buckling problem, each different boundary condition is studied by altering the length to thickness ratio and when necessary, the length to width ratio. Initial tests are done with rotary inertia effects removed from the model. The second runs, with RI re-introduced gives a relative perspective of the importance of shear and inertia in an accurate representation of plate action. Generally speaking, Table 3.4 provides a good idea of the trend observed for all of the vibration problems studied. Rotary inertia is found to decrease the overall stiffness of the plate by an average value of less than one percent. Relative to shear deformation, rotary inertia complicates a plate mathematical model with no important increase in accuracy.

As was the case for the buckling problem, a trend that is observed, regardless of boundary conditions, is the diminished impact of shear deformation as plate length to thickness increases. All curves of ω ($\omega a^2 (\rho/E_2 h^2)^{1/2}$) vs S show a decrease of the discrepancy between SDT and CPT as S increases. Transverse shear variations are inverse functions of plate thickness and become negligible for high enough values of S .

For the plate simply-supported on all sides, a square geometry is used in calculating the natural frequency. Length to thickness is varied from 15.0 to 30.0 and the results are recorded in Figure 3.7. The curve is for the model that included rotary inertia effects. The average difference with/without RI for this problem is 0.19%. A difference of 29.14% exists between SDT and the extrapolated CPT when the length to thickness is 10. This difference drops very quickly as the curves flattens out around S of 32.5.

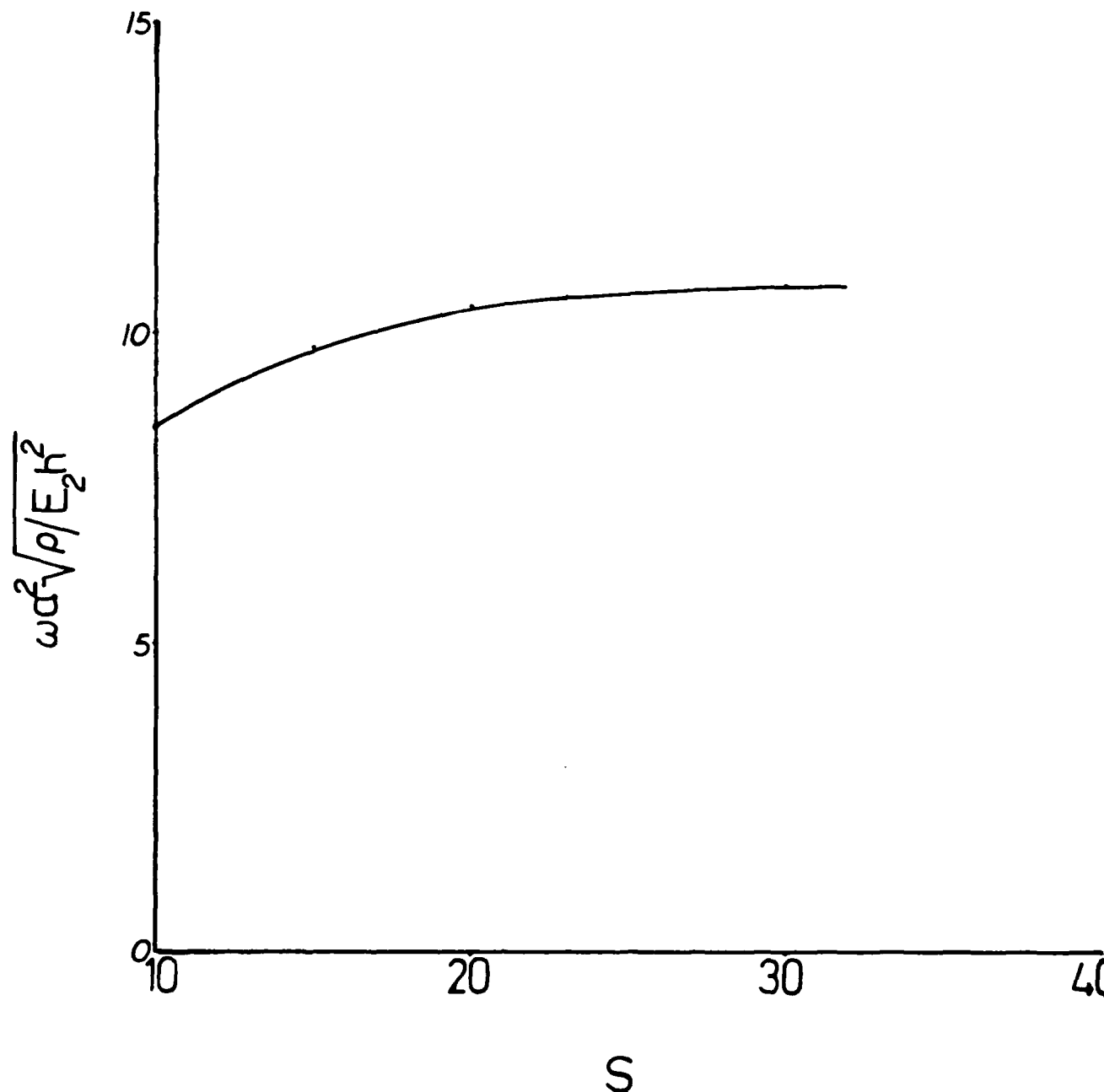


Figure 3.7 Plot of Frequency vs Thickness Ratio
For Simple-Simple Boundaries.

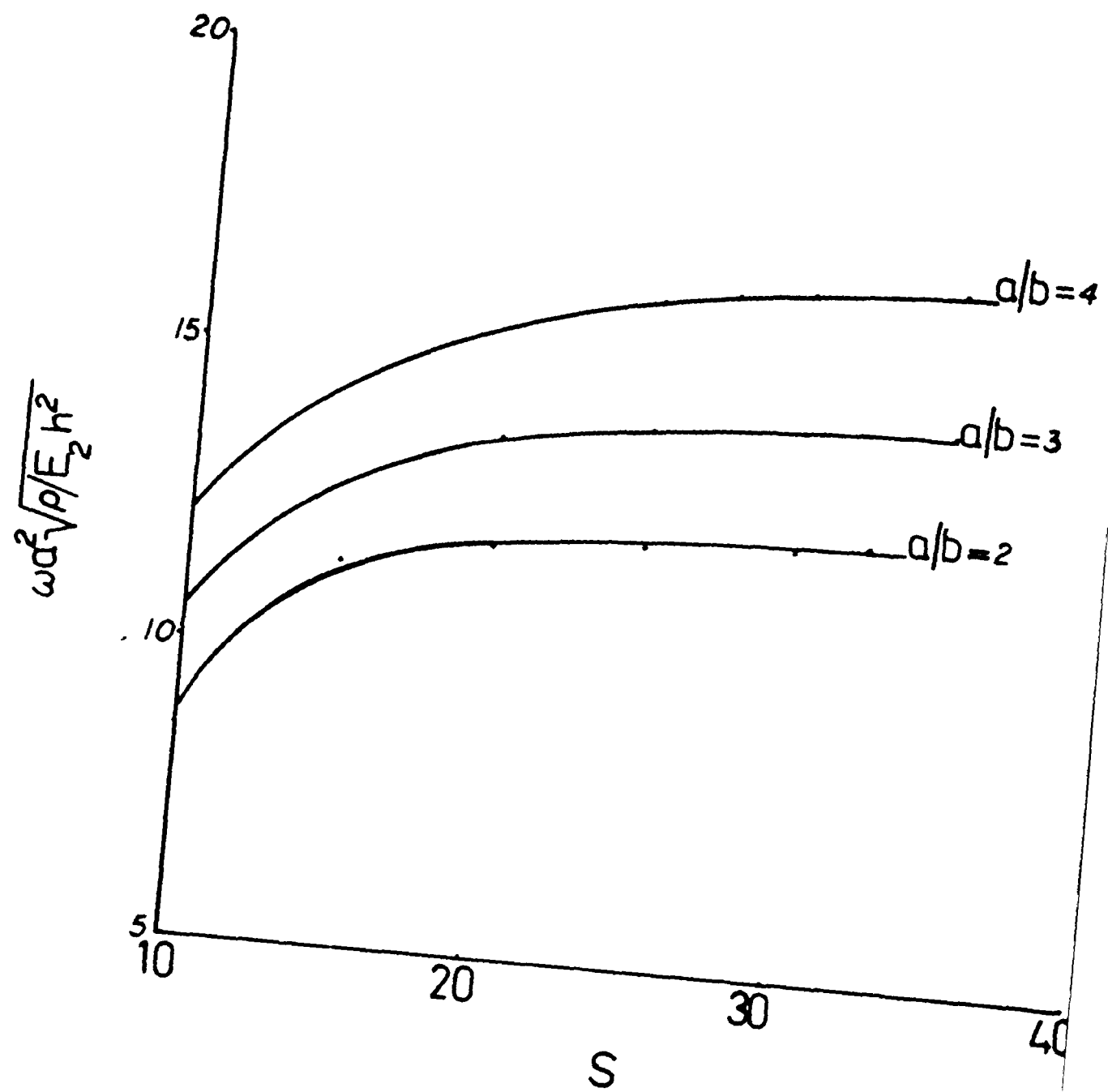


Figure 3.8 Plot of Frequency vs Thickness Ratio
For Clamped-Clamped Boundaries.

A rectangular plate with aspect ratios of two, three, and four is used in the analysis of the clamped-clamped y boundary conditions. As seen in Figure 3.8, S is varied from 15 to 35 for the aspect ratio of two. Maximum deviation between theories is 38.64% for this geometry. Variations of S from 20 to 35 are used in calculations for a/b equal to three. It becomes clear from Figure 3.8 that a narrower plate is stiffer as the natural frequency increases. The plate behaves more and more like a reinforced beam as a/b increases past a ratio of two. Maximum theoretical difference for this configuration is 33.4% for a/b of four, this maximum reaches 34.43% as frequency is plotted for S of 20 to 32.5.

The square plate is once again used to analyze the simple-clamped boundary in y. The curve in Figure 3.9 is valid for S ranging from 15 to 25. Computer limitations prevent the use of larger S values in the computation of the natural frequency. A maximum divergence of 36.4% is recorded for this plate between theory considering shear through the thickness and classical analysis.

For the simple-free y directed boundaries, plate behaviour is depicted in Figure 3.10. A square and a rectangular plate are used to show frequency variations as functions of plate length to thickness ratios. For the square plate, with a variation in S of 17.5 to 22.5, the maximum difference between theories is 16.1%. For the plate with aspect ratio of two and variance of S of 15 to 35, this difference peaks at 20.2%. For this problem, it is interesting to note that an increase of a/b from one to two represents a decrease in plate stiffness.

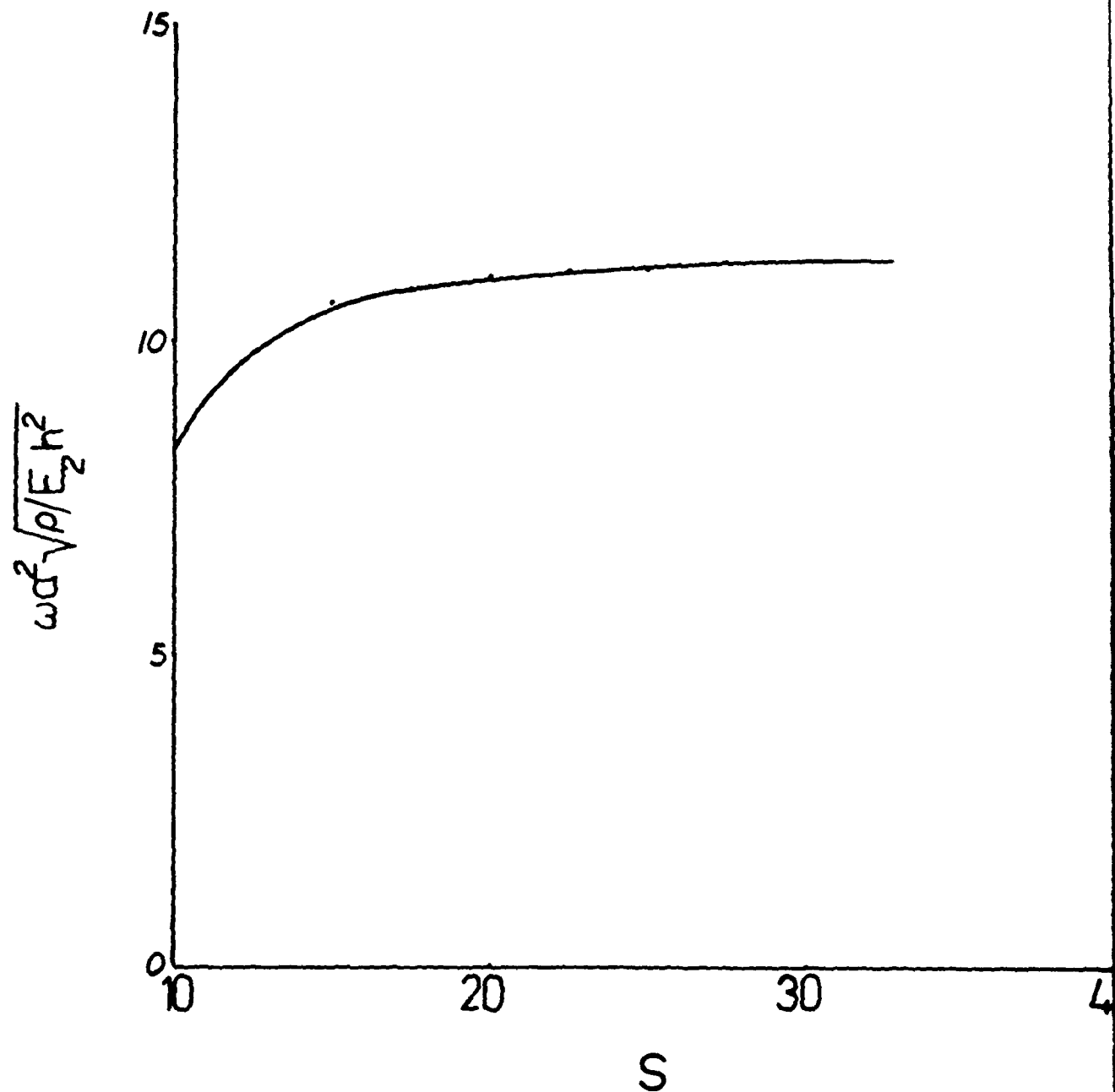


Figure 3.9 Plot of Frequency vs Thickness Ratio
For Simple-Clamped Boundaries.

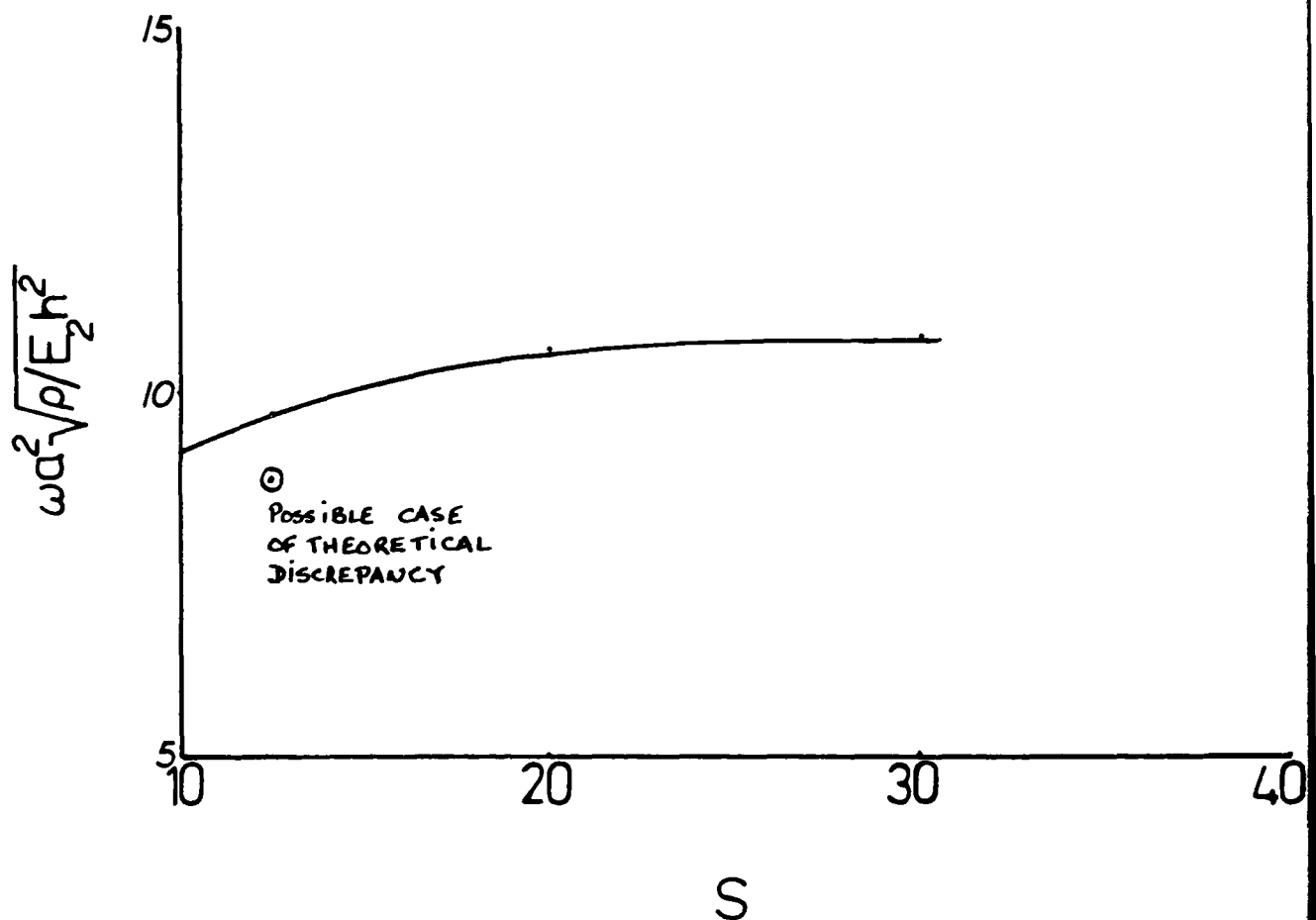


Figure 3.10 Plot of Frequency vs Thickness Ratio
For Simple-Free Boundaries.

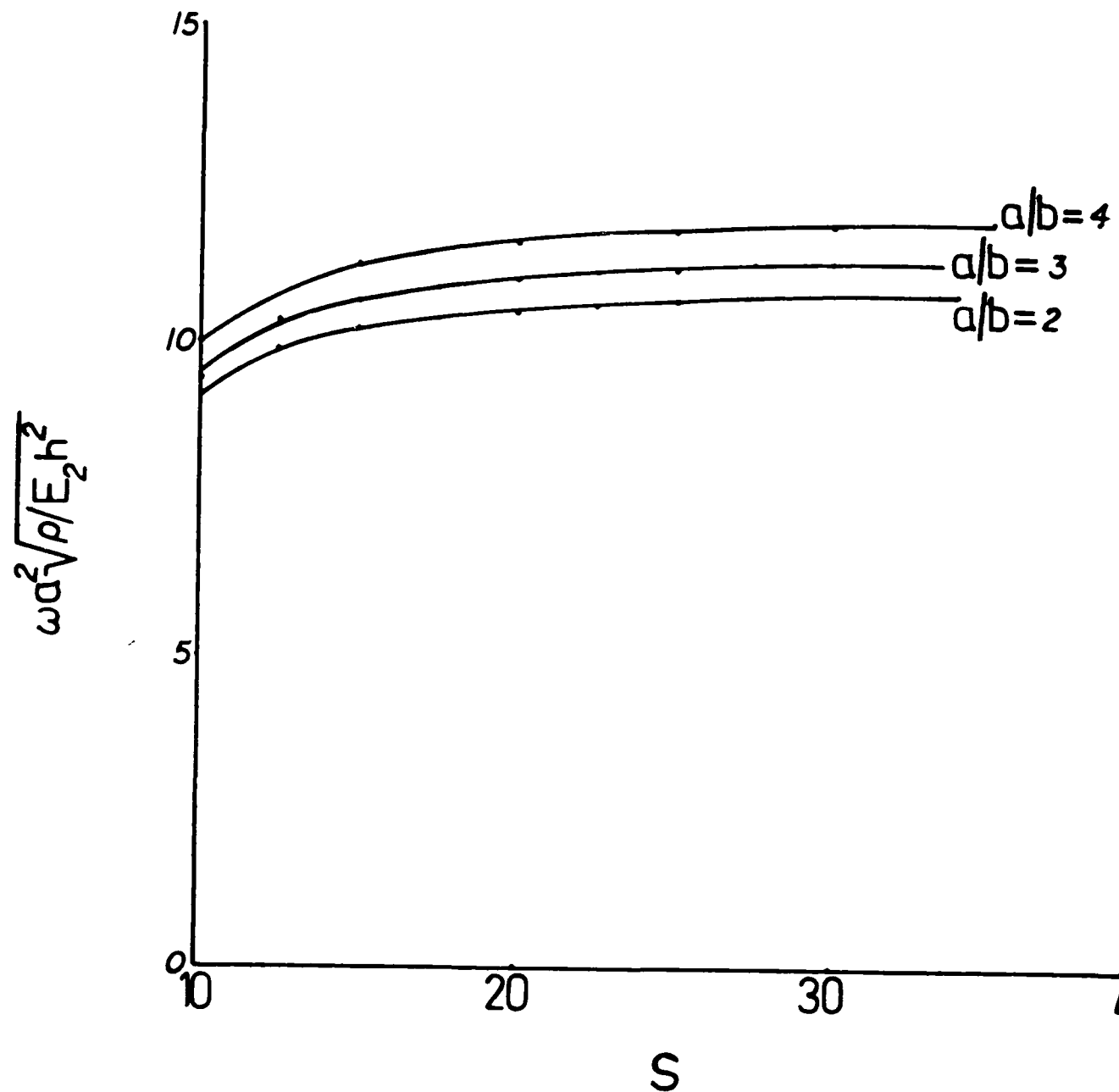


Figure 3.11 Plot of Frequency vs Thickness Ratio
For Clamped-Free Boundaries.

The clamped-free plate, whose behaviour is illustrated in Figure 3.11, is studied for three different aspect ratios. Once again, the influence of shear deformation is very noticeable as is the fact that this influence become negligible quickly as S approaches 40. Maximum differences between classical theory and shear deformation theory vary from 19.44% to 22.16% for aspect ratios of two to four respectively.

Important trends are seen to be slightly different for the vibration problem than those recorded for the buckling problem. First, the overall impact of shear deformation seems to be equivalent for the vibration problem, as illustrated by the values in Table 3.6. Regardless of y boundary conditions, average, difference between SDT and CPT is 27.02% for the vibration problem, very close to the 28.82% obtained for the buckling problem. (In this comparison, RI effects have been excluded for the vibration problem.) The values obtained in Table 3.6 compare normalized frequency at S equal to 10 and 30. For values of S less than 10, the discrepancy between SDT and CPT quickly increases.

Secondly, shear is more important to consider when studying the boundary conditions which are stiffer. The clamped-clamped, simple-clamped and simple-simple have an average difference between the two theories of 34.4%. The boundaries containing a free edge, on the other hand, have an average discrepancy of 19.64%. Thus, the shear force effects are higher when the influence due to rigid plate boundaries is more pronounced.

Boundaries in y	Aspect Ratio of Plate	Max Difference between SDT/CPT (%)
SS	1	29.14
SC	1	36.40
SF	1	16.10
SF	2	20.20
CC	2	38.64
CC	3	33.40
CC	4	34.43
CF	2	19.44
CF	3	20.32
CF	4	22.16

Table 3.6 Comparison of Discrepancies Between Shear Deformation Theory and Classical Plate Theory for Vibration Problems

Thirdly, a quick comparison shows that the stiffness of the boundaries does affect the magnitude of the natural frequency of the plate. The stiffer the supports, the higher the natural frequency of the plate. This can be clearly seen by comparing values of ω for the CC vs the CF plate or the SS vs the SF plate.

Finally, comparison of the two inch plate used in this thesis to the one inch thick plate used by Bowlus [2] indicates a small difference in the maximum discrepancy recorded between SDT and CPT. This is expected as the thicker heavier plate is more affected by force variations through the thickness as they tend to be more pronounced than for a thinner plate.

IV Conclusions

The results obtained from the computations performed in this thesis allow the following conclusions to be presented. They include comments on the Levy technique and on both the stability and vibration problems. It should be noted that all conclusions made are based on the specific laminate used in this thesis. The author does not attempt to generalize the results for laminates of arbitrary compositions nor should the reader.

Levy Technique

1. The Levy technique is a viable means of obtaining base-line solutions for a specific class of laminated composite plates.
2. The mathematics of the solution, especially for free boundaries, is a great deal less algebraically complex than what is generated using a Rayleigh-Ritz or Galerkin approach.
3. The Levy technique cannot be extended to a general class of composite plates. The presence of bending-extensional, bending-twisting coupling terms or D_{16}/D_{26} terms would not allow the reduction of partial differential equations to simple differential equations. Thus, though the Levy method has been around for many years, it has never been fully taken advantage of due to this drawback.
4. The transcendental equations, which are solved for the different boundaries in y , are very sensitive to plate geometry. In many cases, certain length to thickness or length to width problems could not be resolved due to the accuracy limitations of the computer used.

5. Convergence is not a parameter of concern with the Levy procedure. It is not a term dependent approach and consequently, the accuracy of the solution is not dependent on the accuracy of the displacement models.

Buckling Problem

1. As the length to thickness ratio is increased past 40 for the plate, the effects of shear deformation become negligible. Classical plate theory can be used effectively to predict plate behaviour for the thinner plates.
2. Curves of the nondimensionalized buckling load vs thickness ratio are all monotonically increasing as S increases. The rate of increase does vary significantly when different ranges of S are considered. Increase averages 37.6% for S from 10 to 20 and 28.7% for S from 20 to 30 for the boundary conditions.
3. Shear deformation effects account for an average difference of 29.93% between extrapolated classical theory and shear theory. The effect is less pronounced for boundaries conditions which are not very stiff, such as FF.

Vibration Problem

1. Curves for non-dimensionalized natural frequency vs thickness ratio are all monotonically increasing as S increases. Rate of increase does vary along the curve, being the largest for S from 10 to 20 with an average value of 38.8%.
2. Shear deformation effects account for an average difference of 27.02% between extrapolated classical theory and shear theory. The effect is more

pronounced for the boundaries which are stiffer, such as clamped-clamped or simple-clamped.

3. Rotary inertia has very little effect on the overall plate stiffness and can be neglected in the mathematical model of plate behaviour when calculating the first natural frequency. For higher natural frequencies, RI may have significance and should be retained, but this has not been evaluated within this thesis.

Appendix A

BUCKLING ANALYSIS

Matrix [A_{ij}]

$$\begin{bmatrix}
 2 & & & & & & \\
 n^2 & r^2 & 2 & 2 & & & \\
 \hline
 \frac{n^2}{z} + t^2 - n & & -n & & & t & \\
 & & & & & & \\
 & & & & & & \\
 & & 2 & 2 & & & \\
 & & f^2 t^2 & g^2 n^2 & & & \\
 \hline
 -n & & \frac{z^2}{z^2} - \frac{z^2}{z^2} - 1 & & & \frac{e^2 n^2 t^2}{z^2} & \\
 & & z^2 & z^2 & & & \\
 & & & & & & \\
 & & e^2 n^2 t^2 & 2 & 2 & & \\
 & & \frac{z^2}{z^2} - \frac{z^2}{z^2} - 1 & h^2 t^2 & f^2 n^2 & & \\
 & & z^2 & z^2 & z^2 & & \\
 & & & & & & \\
 \end{bmatrix}$$

Commands used to obtain simplified expression for det[A_{ij}]

- 1) determinant(%);
- 2) ratexpand(%);
- 3) xthru(%);
- 4) factor(%);
- 5) * by z**3/fhz;

Expression for the determinant of [A_{ij}].

$$\begin{aligned}
 & \left(\frac{n^2}{z} + t^2 - n^2 \right) \left(\frac{f^2 t^2}{z^2} - \frac{g^2 n^2}{z^2} - 1 \right) \left(\frac{h^2 t^2}{z^2} - \frac{f^2 n^2}{z^2} - 1 \right) + \frac{e^2 n^2 t^2}{z^2} \\
 & + n^2 \left(\frac{e^2 n^2 t^2}{z^2} - n^2 \left(\frac{h^2 t^2}{z^2} - \frac{f^2 n^2}{z^2} - 1 \right) \right) + t^2 \left(t^2 \left(\frac{f^2 t^2}{z^2} - \frac{g^2 n^2}{z^2} - 1 \right) + \frac{e^2 n^2 t^2}{z^2} \right)
 \end{aligned}$$

Simplified expression for the determinant of $[A_{ij}]$.

$$\begin{aligned}
 & (-h^2 t^2 z^2 + 2 f n^2 t^2 z^2 + 2 e n^2 t^2 z^2 + n^2 r^2 z^2 - g n^2 z^2 \\
 & - g^2 h^2 n^2 t^2 z^2 - f h n^2 t^2 z^2 - f^2 n^2 t^2 z^2 + e^2 n^2 t^2 z^2 - h^2 n^2 r^2 t^2 z^2 \\
 & - f^2 n^2 r^2 t^2 z^2 + g h n^2 t^2 z^2 + f g n^2 t^2 z^2 + f^2 n^2 t^2 z^2 - e^2 n^2 t^2 z^2 \\
 & + f^4 n^2 r^2 z^2 - f g n^2 z^2 + f h n^2 r^2 t^2 z^2 - g h n^2 r^2 t^2 z^2 - f^2 n^2 r^2 t^2 z^2 \\
 & + f g n^2 r^2 z^2 + f h t^2 z^2 + g n^2 r^2 z^2 + e^2 n^2 r^2 t^2 z^2) / (f h z)
 \end{aligned}$$

Expressions for A_j in Equation(63).

$$A_3 = f h z / f h z = 1.0$$

$$A_2 = (-h z^2 - g h n^2 z^2 - f h n^2 z^2 - f^2 n^2 z^2 + e^2 n^2 z^2 + f h n^2 r^2 z^2) / f h z$$

$$\begin{aligned}
 A_1 = & (2 f n^2 z^2 + 2 e n^2 z^2 - h n^2 r^2 z^2 - f n^2 r^2 z^2 + g h n^2 z^2 + f g n^2 z^2 + f^2 n^2 z^2 - e^2 n^2 z^2 \\
 & - g h r n^2 z^2 - f^2 n^2 r^2 z^2 + e^2 r n^2 z^2) / f h z
 \end{aligned}$$

$$A_0 = (n^2 z^2 r^2 + g z r n^2 z^2 + f z r n^2 z^2 + f g r n^2 z^2 - g z^2 n^2 z^2 - f g r n^2 z^2) / f h z$$

Appendix B

VIBRATION ANALYSIS

Matrix $[A_{ij}]$

$$\begin{bmatrix}
 y & 2 & 2 \\
 - + t - n & - n & t \\
 z & & \\
 & & \\
 - n & x & f t & g n & e n t \\
 - + \frac{2}{z} - \frac{2}{z} - 1 & z & z & z & z \\
 & & & & \\
 - t & e n t & x & h t & f n & \\
 - \frac{2}{z} & z & z & z & z & - 1
 \end{bmatrix}$$

Commands used to obtain simplified expression for $\det[A_{ij}]$:

- 1) determinant(%);
- 2) ratexpand(%);
- 3) xthru(%);
- 4) factor(%);
- 5) * by z**3/fhz;

Expression for the determinant of $[A_{ij}]$.

$$\begin{aligned}
 & \frac{y^2 z^2}{(- + t - n)^2} \frac{x^2 f^2 t^2 g^2 n^2}{z^2 z^2 z^2} \frac{x^2 h^2 t^2 f^2 n^2}{z^2 z^2 z^2} e^{- \frac{2}{z} - \frac{2}{z} - 1} + \\
 & + n \frac{e^2 n^2 t^2}{z^2} \frac{x^2 h^2 t^2 f^2 n^2}{z^2 z^2 z^2} e^{- \frac{2}{z} - \frac{2}{z} - 1} + t (t - \frac{2}{z}) e^{- \frac{2}{z} - \frac{2}{z} - 1} + \\
 & + \frac{e^2 n^2 t^2}{z^2}
 \end{aligned}$$

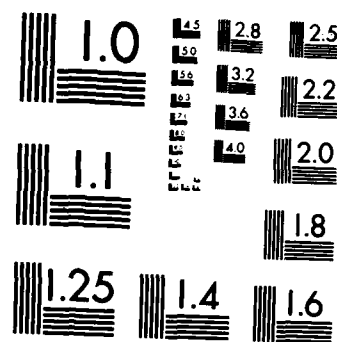
AD-A189 743

THE BUCKLING AND VIBRATION OF COMPOSITE PLATES USING
THE LEVY METHOD CONS (U) AIR FORCE INST OF TECH
WRIGHT-PATTERSON AFB OH SCHOOL OF ENGI R F PALARDY
UNCLASSIFIED DEC 87 AFIT/GAE/RA/87D-16 F/G 11/4

2/2

NL





MICROCOPY RESOLUTION TEST CHART
NATIONAL BUREAU OF STANDARDS-1963-A

Simplified expression for the determinant of $[A_{ij}]$.

$$\begin{aligned}
 & (y^2 z^2 - t^2 x z^2 + n^2 x z^2 - h^2 t^2 z^2 + 2 f n t^2 z^2 + 2 e n t^2 z^2 \\
 & - g n^2 z^2 - 2 x y z^2 - h^2 t^2 y z^2 - f t^2 y z^2 + g n^2 y z^2 + f n^2 y z^2 \\
 & - n^2 x^2 z^2 + h^2 t^2 x^2 z^2 + f t^2 x^2 z^2 - h n^2 t^2 x^2 z^2 - g n^2 t^2 x^2 z^2 \\
 & + g n^4 x^2 z^2 + f n^4 x^2 z^2 + f h t^4 z^2 - g h n^2 t^2 z^2 - f h n^2 t^2 z^2 \\
 & + e n^2 t^4 z^2 + g h n^2 t^4 z^2 + f g n^2 t^4 z^2 + f n^2 t^4 z^2 - e n^2 t^4 z^2 \\
 & + x^2 y^2 + h t^2 x^2 y^2 + f t^2 x^2 y^2 - g n^2 x^2 y^2 - f n^2 x^2 y^2 + f h t^2 y^2 \\
 & - f n^2 t^2 y^2 + e n^2 t^2 y^2 + f g n^2 y^2 + t^2 x^2 z^2 - 2 f n^2 t^2 x^2 z^2 \\
 & - f n^2 t^4 z^2 - f g n^2 z^2 - g h n^2 t^4 y^2) / (f h z)
 \end{aligned}$$

Expressions for B_j in Equation(81).

$$B_3 = f h z / f h z = 1.0$$

$$\begin{aligned}
 & B_2 = (-h z^2 + h x z^2 + f x z^2 - g h n^2 z^2 - f h n^2 z^2 - f n^2 z^2 + e n^2 z^2 + f h y^2) / f h z \\
 & B_1 = (-x z^2 + 2 f n^2 z^2 + 2 e n^2 z^2 - h y z^2 - f y z^2 + x z^2 - g n^2 x z^2 - 2 f n^2 x z^2 + g h z n^2 + \\
 & f g z n^2 + f z n^2 - e z n^2 + h x y^2 + f x y^2 - g h n^2 y^2 - f n^2 y^2 + e n^2 y^2) / f h z \\
 & B_0 = (y z^2 + n^2 x z^2 - g z n^2 - 2 x y z^2 + g y z n^2 + f n^2 y z^2 - n^2 x z^2 + g x z n^2 + f x z n^2 - f g z n^2 + \\
 & x^2 y^2 - g n^2 x y^2 - f n^2 x y^2 + f g y n^2) / f h z
 \end{aligned}$$

Appendix C

Appendix C

The first program is a fortran rewrite of a basic program used by Bowlus [2] to determine the nondimensional stiffnesses of a laminated plate. In particular, the program is rewritten to specifically handle $[0/90]_{ms}$ ply layups and no other as this is the only type of plate studied in this thesis. The program has four main sections; the input, the computation of lamina stiffnesses, the computation of the laminate stiffnesses and the output. The input obtains the following

- a) plate top and bottom dimensions
- b) E_1 , E_2 , G_{12} , ν_{12} and mass density for laminate material
- c) number of plies in laminate

Based on this information and the fact that only $[0,90]_{ms}$ laminates are considered, a do-loop is employed to calculate the non-dimensional lamina stiffnesses $[Q_{ij}]_k$. An "ms" laminate means the first $m/4$ lamina are oriented at 0° , the next $m/2$ at 90° and the last $m/4$ at 0° . This allows the use of a simplifying do-loop. Once a lamina $[Q_{ij}]_k$ is calculated, it is added to the sum of the other $k-1$ lamina stiffnesses and the $k+1$ stiffnesses are calculated. Doing this m times gives the non-dimensional laminate stiffnesses $[Q_{ij}]$. The second and third sections of the program completes these steps. The output is presented to the user in the form of a table which gives the type of laminate studied and a listing of the non-dimensional stiffnesses calculated.

```

***** ****
*** Program to compute the extensional and bending
***** stiffness elements for a symmetric laminate
***** build-up, given lamina properties.
***** ****

      write(6,10)
10      format('enter plate top & bot dimensions,use 2f10.5',/)
      read(5,15) ztop,zbot
15      format(2f10.5)
c
c      section to obtain lamina data
c
17      write(6,20)
20      format('enter E1,E2,G12,v12 and mass density',/)
      write(6,30)
30      format('use 3e10.2 and 2f7.3, OK?',/)
      read(5,40) E1,E2,G1,V1,rho
40      format(3e10.2,2f7.3)
45      write(6,50)
50      format('how many plies in this plate,use I3',/)
      read(5,60) n
60      format(I3)
      V2=V1*(E2/E1)
      G3=G1
      G2=0.8*G1
      a1=0.0
      a2=0.0
      d1=0.0
      d2=0.0
      d3=0.0
      d4=0.0
      ps=0.0
c
c      section to compute A and D elements for this ply
c
      Q1=E1/(1.0-(V1*V2))
      Q2=(V1*E2)/(1.0-(V1*V2))
      Q3=E2/(1-(V1*V2))
      Q4=G2
      Q5=G3
      Q6=G1
      tk=(ztop-zbot)/n
      k=n/4
      DO 100 I=1,n
         if(I.gt.k) go to 80
70      th=0.0
         go to 90
80      if(I.gt.3*k) go to 70
         th=3.1415927/2.0
c
c      section to compute QBARS
c
90      B1=Q1*((COS(TH))**4+2.0*(Q2+2.0*Q6)*(SIN(TH))**2*
*          (COS(TH))**2+Q3*(SIN(TH))**4
      B2=(Q1+Q3-4.0*Q6)*(SIN(TH))**2*(COS(TH))**2+
*          Q2*((SIN(TH))**4+(COS(TH))**4)
      B3=Q1*((SIN(TH))**4+2.0*(Q2+2.0*Q6)*(SIN(TH))**2*

```

```

*      (COS(TH))**2+Q3*(COS(TH))**4
B4=(Q1+Q3-2.0*Q2-2.0*Q6)*(SIN(TH))**2*(COS(TH))**2
*      +Q6*((SIN(TH))**4+(COS(TH))**4)
B5=Q4*(COS(TH))**2+Q5*(SIN(TH))**2
B6=Q5*(COS(TH))**2+Q4*(SIN(TH))**2
c
c      section to compute lamina A elements
c
      Z1=ztop-I*tk
      ZK=ztop-(I-1)*tk
      A3=B5*(ZK-Z1)
      A4=B6*(ZK-Z1)
      F=RHO*(ZK-Z1)
c
c      section to compute lamina D elements
c
      DZ=(ZK**3-Z1**3)/3.0
      F1=B1*DZ
      F2=B2*DZ
      F3=B3*DZ
      F4=B4*DZ
c
c      section to find laminate A and D elements
c
      A1=A1+A3
      A2=A2+A4
      D1=D1+F1
      D2=D2+F2
      D3=D3+F3
      D4=D4+F4
      PS=PS+F
100    continue
c
c      section to print out A and D elements of laminate
c
      write(6,200)
200    format(26x,'graphite-epoxy [0,90]',/,46x,'2s',//,
*32x,'one inch thick',///,21x,'element',4x,
*'dimensional value',///)
      write(6,300) A1,A2,D1,D2,D3,D4
300    format(23x,'A44',10x,F13.4,///,23x,'A55',10x,
*F13.4,///,23x,'D11',10x,F13.4,///,23x,'D12',10x,
*F13.4,///,23x,'D22',10x,F13.4,///,23x,'D66',
*10x,F13.4,///,'Units for Aij terms are lb/in',
*///,'Units for Dij terms are in-lbs',//)
      write(6,350)
350    format('another problem maybe? yes=1,no=2',/)
      read(5,360) j
360    format(I1)
      if(j.eq.2) go to 400
      write(6,370)
370    format('same physical pro. but diff. # plies? yes=1',/)
      read(5,380) m
380    format(I1)
      if(m.eq.1) go to 45
      go to 17
400    stop
      end

```

Appendix D

Appendix D

This second program, also written in Fortran, has four main sections. The transcendental equations in the fourth section of this program are solved using the incremental search technique. A flowchart describing the mechanics of this technique is included in Appendix E. The four sections of the program are; the input, the calculation of the coefficients of the sixth order equation in θ , Eq. (63), the evaluation of α , β , γ , and related values such as $\Lambda(\alpha)$, and the solution of the transcendental equation for a particular set of boundaries in y .

The input section obtains the following data:

- a) number of modes, n , calculations are to be repeated for
- b) a/b ratio of the plate
- c) does user want to include effects of shear deformation
and/or rotary inertia in calculations?
- d) the boundary conditions in y
- e) buckling or vibration problem ?

The following are an intrinsic part of the program but can of course be altered by editing the source code:

- a) the material properties of the plate under investigation
- b) a/h ratio used in calculation (automatically varied from 10 to 50 for each a/b ratio inputed)
- c) initial and final values of eigenvalue, initial increment
for eigenvalue and answer tolerance (all parameters
required when using incremental search)

Depending on the type of problem being solved, the second section of the program calculates the coefficients of Eq. (63). Subroutines are used for this purpose and appropriate terms are omitted if, in the vibration analysis, rotary inertia is removed. Values returned are used in the third section to calculate α , β , and γ , and all other terms required to define the displacements. These terms are defined by Eqs. (69), (70), (72), (73), (82), (83), (84), and (85).

The expressions for the transcendental equations, computed in the previous section of the thesis and subsequently encoded, are evaluated in the final section of the program. An eigenvalue, for the particular problem under consideration, is obtained when the transcendental expression is identically zero. In using this program, one should realize that certain limitations to the plate geometries, which may be studied, do exist. These limitations are either computational or theoretical in origin. For each boundary condition in y studied in the thesis, the range of S used in the calculations and the aspect ratio of the plate are specified. These provide the user with a very good approximation of the useful computational limits of this program.

Inconsistencies present in the theory can best be identified by examining the graphical results and observing deviations from the general trend. As was discussed earlier, some deviations may result from the assumption that all roots to Eq. (65) are real. Neglecting the complex conjugate roots is a good simplification as only two instances occur, in all computation, where the roots appear to be complex. A second source of deviation occurs when a very thick plate, S around ten, is studied. In this case, the assumptions of plane stress and no strain in the z direction may lead to errors which are no longer negligible, depending on the boundary

conditions. Such deviations, did occur twice, both times for S less than 15 and are identified on the appropriate figures. Thus, the theory is inexact but more than adequate for the problems studied in this thesis.

```

c ****
c Program to obtain uniaxial buckling load for a square
c composite plate given boundary conditions. Program can
c also calculate the natural frequencies of such a plate.
c ****
      DIMENSION deter(2),A(3),KAPA(3),KAPA1(3),OMEGA(3),OMEGA1(3)
      REAL NU,n
      INTEGER type,bc,pp,sd
      DOUBLE PRECISION aa,thick,r,w,coeft4,coeft2,coeft0,e,f,g,
*h,z,x,b,c,d,p,q,ALPHA,BETA,GAMMA,A,KAPA,bb,v1,v2,v3,v4,
*v5,v6,v7,v8,pi,BIGB,U,VE,ALPHA2,BETA2,GAMMA2,KAPA1,
*det,DIS,rho,a11,a12,a13,a21,a22,a23,a31,a32,a33,OMEGA,
*OMEGA1,eigen,xmax,dxi,epsi,deltx,v9,v10,v11,v12,v13,v14,o
*E2,answer
      COMMON /A/A44,D12,D66,D11,D22,m,aa
c Material properties for a composite plate 2" thick.
4      A44=1080000.625
      D11=12441315.0
      D12=281690.125
      D22=2582159.0
      D66=400000.0
      rho=0.055
      E2=1.40d06
      write(6,6)
6      format('remember, this plate is 2" thick!',/)
10     write(6,40)
40     format('how many modes problem to be solved for?,use I1')
      read(5,50) mm
c The user must choose for how many modes he wants to solve
c a particular a/h & a/b geometry for.
50     format(I1)
      write(6,60)
60     format('problem to be solved?buckling=1,vibs=2')
      read(5,70) type
70     format(I1)
      write(6,80)
80     format('what is a/b & thickness of the plate?')
      write(6,90)
90     format('use 2f8.3 to input values,okay?')
      read(5,100) ab,thick
100    format(2f8.3)
      write(6,103)
103    format('do you want to include SD? yes=1,no=2')
      read(5,106) sd
106    format(I1)
      write(6,110)
110    format('do you want to include RI? yes=1, no=2')
      read(5,120) L
120    format(I1)
      write(6,125)
125    format('what BC's do you want for y=0,b ?',/)
      write(6,130)
130    format('SS=1,CC=2,SC=3,SF=4,CF=5,FF=6',/)
      read(5,135) bc
135    format(I1)
      aaa=10.0
140    m=1

```

EVALUATION OF 3 REAL ROOTS OF EQN (65) OR EQN(81)

```

        if(GAMMA2.lt.0.) GAMMA2=-1.*GAMMA2
        ALPHA=dsqrt(ALPHA2)
        BETA=dsqrt(BETA2)
        GAMMA=dsqrt(GAMMA2)
        if(type.eq.2) go to 650
        do 550 J=1,3
c Buckling Problem
c if one of the roots of the cubic is negative, then eqs(72)
c and (73) must be used instead of eqs(69) and (70).
        if(A(J).lt.0.) go to 530
c eq(69) and eq(70) follow:
        KAPA(J)=((h*A(J)-z-n*n*f)*n*z-n*e*z*A(J))
        * /((h*A(J)-z-n*n*f)*(f*A(J)-z-n*n*g) +
        * n*n*e*e*A(J))
        if(J.eq.1) angle=ALPHA
        if(J.eq.2) angle=BETA
        if(J.eq.3) angle=GAMMA
        KAPA1(J)=(n*z-(f*A(J)-z-n*n*g)*KAPA(J))/(n*e*angle)      EQN.(69)
        go to 550
c eq(72) and eq(73) follow:
530   KAPA(J)=((h*A(J)+n*n*f+z)*n*z-n*e*z*A(J))
        * /((n*n*e*e*A(J)-(h*A(J)+n*n*f+z)*(f*A(J)+n*n*g+z))
        if(J.eq.1) angle=ALPHA
        if(J.eq.2) angle=BETA
        if(J.eq.3) angle=GAMMA
        KAPA1(J)=(n*z+(f*A(J)+n*n*g+z)*KAPA(J))/(n*e*angle)      EQN.(70)
550   continue
        go to 700
650   do 685 JJ=1,3
c Vibration Problem
c if one of the roots of the cubic is negative, then eqs(84)
c and (85) must be used instead of eqs(82) and (83).
        if(A(JJ).lt.0.) go to 660
c eq(82) and eq(83) follow:
        OMEGA(JJ)=((h*A(JJ)-z-n*n*f+x)*n*z-n*e*z*A(JJ))
        * /((h*A(JJ)-z-n*n*f+x)*(f*A(JJ)-z-n*n*g+x) +
        * n*n*e*e*A(JJ))
        if(JJ.eq.1) angle=ALPHA
        if(JJ.eq.2) angle=BETA
        if(JJ.eq.3) angle=GAMMA
        OMEGA1(JJ)=(n*z-(f*A(JJ)-z-n*n*g+x)*OMEGA(JJ))/      EQN.(82)
        * (n*e*angle)
        go to 685
c eq(84) and eq(85) follow:
660   OMEGA(JJ)=((h*A(JJ)+n*n*f+z-x)*n*z-n*e*z*A(JJ))
        * /((n*n*e*e*A(JJ)-(h*A(JJ)+n*n*f+z-x)*(f*A(JJ)+n*n*g+z-x))      EQN.(84)
        if(JJ.eq.1) angle=ALPHA
        if(JJ.eq.2) angle=BETA
        if(JJ.eq.3) angle=GAMMA
        OMEGA1(JJ)=(n*z+(f*A(JJ)+n*n*g+z-x)*OMEGA(JJ))/      EQN.(85)
        * (n*e*angle)
685   continue
c ****
c Start of fourth section of program.
c solution to transcendental equation of boundary-value problem.
c ****
700   go to (960,1000,1100,1200,1300,1400) bc

```

```

750  deter(k)=det
      if(k.eq.2) go to 790
      k=k+1
755  eigen=eigen+deltx
      go to 146
790  if(deter(1)*deter(2)) 800,820,795
795  if(eigen.gt.xmax) go to 850
      deter(1)=deter(2)
      go to 755
800  if(deltx-epsi) 820,820,810
810  eigen=eigen-deltx
      deltx=deltx/10.
      go to 755
820  if(type.eq.2) go to 825
      answer=eigen*bb*bb/(pi*pi*aa*sqrt(g*h))
      go to 827
825  answer=eigen
827  write(6,830) aa,bb,m,answer
830  format('aa=',f8.3,x,'bb=',f8.3,x,'n=',I1,x,'root=',d20.10,/)
      go to 890
850  write(6,860)
860  format('max value reached and no root found',/)
890  if(m.ge.mm) go to 895
      m=m+1
      go to 145
895  if(aaa.ge.45.0) go to 899
      aaa=aaa+2.5
      go to 140
899  write(6,900)
900  format('do you want to try another problem?yes=1')
      read(5,910)J
910  format(I1)
      if(j.ne.1) go to 950
      write(6,920)
920  format('any change in mat'l properties? y=1',/)
      read(5,930) pp
930  format(I1)
      if(pp.eq.1) go to 4
      go to 10
950  stop
960  if(a(2).gt.0.0) go to 970
c Routine to calculate det[aij] for "simple-simple" bc in y.
      det=beta-pi/bb
      go to 750
970  if(type.eq.2) go to 980
      v1=kapa(1)
      v2=kapa(2)
      v3=kapa(3)
      v4=kapa1(1)
      v5=kapa1(2)
      v6=kapa1(3)
      go to 990
980  v1=omega(1)
      v2=omega(2)
      v3=omega(3)
      v4=omegal(1)
      v5=omegal(2)

```

```

      v6=omega1(3)
990   a11=(dsinh(alpha*bb))/1.d10
      a12=(dsinh(beta*bb))/1.d10
      a13=(dsinh(gamma*bb))/1.d10
      a21=(v1*dsinh(alpha*bb))/1.d10
      a22=(v2*dsinh(beta*bb))/1.d10
      a23=(v3*dsinh(gamma*bb))/1.d10
      a31=(v4*alpha*dsinh(alpha*bb))/1.d10
      a32=(v5*beta*dsinh(beta*bb))/1.d10
      a33=(v6*gamma*dsinh(gamma*bb))/1.d10
      det=a11*(a22*a33-a32*a23)-a12*(a21*a33-a31*a23)-
*a13*(a21*a32-a31*a22)
      go to 750
      stop
1000  if(type.eq.2) go to 1010
c  Routine to calculate det[Aij] for "clamped-clamped" bc in y.
      v1=KAPA(1)
      v2=KAPA(2)
      v3=KAPA(3)
      v4=KAPA1(1)
      v5=KAPA1(2)
      v6=KAPA1(3)
      v7=(v1-v3)/(v3-v2)
      v8=(v2-v1)/(v3-v2)
      go to 1020
1010  v1=OMEGA(1)
      v2=OMEGA(2)
      v3=OMEGA(3)
      v4=OMEGA1(1)
      v5=OMEGA1(2)
      v6=OMEGA1(3)
      v7=(v1-v3)/(v3-v2)
      v8=(v2-v1)/(v3-v2)
1020  a11=(dsinh(ALPHA*bb)-v4/v6*dsinh(GAMMA*bb))/1.d10
      a12=(dcosh(ALPHA*bb)+v7*dcos(BETA*bb)
*+v8*dcosh(GAMMA*bb))/1.d10
      a13=(dsin(BETA*bb)+v5/v6*dsinh(GAMMA*bb))/1.d10
      a21=(v1*dsinh(ALPHA*bb)-v3*v4/v6*dsinh(GAMMA*bb))/1.d10
      a22=(v1*dcosh(ALPHA*bb)+v2*v7*dcos(BETA*bb)
*+v3*v8*dcosh(GAMMA*bb))/1.d10
      a23=(v2*dsin(BETA*bb)+v3*v5/v6*dsinh(GAMMA*bb))/1.d10
      a31=(v4*(dcosh(ALPHA*bb)-dcosh(GAMMA*bb)))/1.d10
      a32=(v4*dsinh(ALPHA*bb)+v5*v7*dsin(BETA*bb)
*+v6*v8*dsinh(GAMMA*bb))/1.d10
      a33=(v5*(-dcos(BETA*bb)+dcosh(GAMMA*bb)))/1.d10
      det=a11*(a22*a33-a32*a23)-a12*(a21*a33-a31*a23)-
*a13*(a21*a32-a31*a22)
      go to 750
      stop
1100  if(type.eq.2) go to 1110
c  Routine to calculate det[Aij] for "simple-clamped" bc's in y.
      v1=kapa(1)
      v2=kapa(2)
      v3=kapa(3)
      v4=kapa1(1)
      v5=kapa1(2)
      v6=kapa1(3)

```

```

        go to 1120
1110  v1=omega(1)
        v2=omega(2)
        v3=omega(3)
        v4=omega1(1)
        v5=omega1(2)
        v6=omega1(3)
1120  if(a(2).lt.0.0) go to 1130
        v20=dsinh(beta*bb)
        v30=dcosh(beta*bb)
        go to 1140
1130  v20=dsin(beta*bb)
        v30=-dcos(beta*bb)
1140  a11=(dsinh(alpha*bb))/1.d10
        a12=(v20)/1.d10
        a13=(dsinh(gamma*bb))/1.d10
        a21=(v1*dsinh(alpha*bb))/1.d10
        a22=(v2*v20)/1.d10
        a23=(v3*dsinh(gamma*bb))/1.d10
        a31=(v4*dcosh(alpha*bb))/1.d10
        a32=(v5*v30)/1.d10
        a33=(v6*dcosh(gamma*bb))/1.d10
        det=a11*(a22*a33-a32*a23)-a12*(a21*a33-a31*a23)-
* a13*(a21*a32-a31*a22)
        go to 750
        stop
1200  if(type.eq.2) go to 1210
c   Routine to calculate det[Aij] for "simple-free" bc's in y.
        v1=kapa(1)
        v2=kapa(2)
        v3=kapa(3)
        v4=kapa1(1)
        v5=kapa1(2)
        v6=kapa1(3)
        go to 1220
1210  v1=omega(1)
        v2=omega(2)
        v3=omega(3)
        v4=omega1(1)
        v5=omega1(2)
        v6=omega1(3)
1220  a11=((h*alpha*v4-n*v1*(e-f))*dsinh(alpha*bb))/1.d10
        a12=((h*beta*v5-n*v2*(e-f))*dsin(beta*bb))/1.d10
        a13=((h*gamma*v6-n*v3*(e-f))*dsinh(gamma*bb))/1.d10
        a21=((alpha*v1+n*v4)*dcosh(alpha*bb))/1.d10
        a22=((beta*v2-n*v5)*dcos(beta*bb))/1.d10
        a23=((gamma*v3+n*v6)*dcosh(gamma*bb))/1.d10
        a31=((alpha+v4)*dcosh(alpha*bb))/1.d10
        a32=((beta-v5)*dcos(beta*bb))/1.d10
        a33=((gamma+v6)*dcosh(gamma*bb))/1.d10
        det=a11*(a22*a33-a32*a23)-a12*(a21*a33-a31*a23)-
* a13*(a21*a32-a31*a22)
        go to 750
        stop
1300  if(type.eq.2) go to 1310
c   Routine to calculate det[Aij] for "clamped-free" bc's in y.
        v1=kapa(1)

```

```

        v2=kapa(2)
        v3=kapa(3)
        v4=kapai(1)
        v5=kapai(2)
        v6=kapai(3)
        v7=(v1-v3)/(v3-v2)
        v8=(v2-v1)/(v3-v2)
        go to 1320
1310  v1=omega(1)
        v2=omega(2)
        v3=omega(3)
        v4=omega1(1)
        v5=omega1(2)
        v6=omega1(3)
        v7=(v1-v3)/(v3-v2)
        v8=(v2-v1)/(v3-v2)
1320  a11=(((-n*(e-f)*v1+h*alpha*v4)*dsinh(alpha*bb) +
        *(v3*v4/v6+n*(e-f)-h*v4*gamma)*dsinh(gamma*bb))/1.d10
        a12=(((-n*(e-f)*v1+h*alpha*v4)*dcosh(alpha*bb) +
        *(-n*(e-f)*v2+h*beta*v5)*v7*dcos(beta*bb) +
        *(-n*(e-f)*v3+h*gamma*v6)*v8*dcosh(gamma*bb))/1.d10
        a13=(((-n*(e-f)*v2+h*beta*v5)*dsin(beta*bb) +
        *(-n*(e-f)*v3*v5/v6+h*gamma*v5)*dsinh(gamma*bb))/1.d10
        a21=((alpha*v1+n*v4)*dcosh(alpha*bb)-
        *(gamma*v3*v4/v6+v4)*dcosh(gamma*bb))/1.d10
        a22=((alpha*v1+n*v4)*dsinh(alpha*bb)-(beta*v2+n*v5)*v7* +
        *dsin(beta*bb)+(gamma*v3+n*v6)*v8*dsinh(gamma*bb))/1.d10
        a23=((beta*v2-n*v5)*dcos(beta*bb) +
        *(gamma*v3*v5/v6+n*v5)*dcosh(gamma*bb))/1.d10
        a31=((alpha+v4)*dcosh(alpha*bb)-(gamma*v4/v6+v4)*
        *dcosh(gamma*bb))/1.d10
        a32=((alpha+v4)*dsinh(alpha*bb)+(-beta+v5)*v7* +
        *dsin(beta*bb)+(gamma+v6)*v8*dsinh(gamma*bb))/1.d10
        a33=((beta-v5)*dcos(beta*bb)+(gamma*v5/v6+v5)*
        *dcosh(gamma*bb))/1.d10
        det=a11*(a22*a33-a32*a23)-a12*(a21*a33-a31*a23) +
        *a13*(a21*a32-a31*a22)
        go to 750
        stop
1400  if(type.eq.2) go to 1410
c  Routine to calculate det[ai,j] for "free-free" bc's in y.
        v1=kapa(1)
        v2=kapa(2)
        v3=kapa(3)
        v4=kapai(1)
        v5=kapai(2)
        v6=kapai(3)
        go to 1420
1410  v1=omega(1)
        v2=omega(2)
        v3=omega(3)
        v4=omega1(1)
        v5=omega1(2)
        v6=omega1(3)
1420  v7=-(n*v4+v1)/(v3+n*v6)
        if (a(2).gt.0.) go to 1430
        v8=(n*v5-v2)/(n*v6+v3)

```

```

        v9=(v4+alpha)+(v6+gamma)*v7
        v10=(beta-v5)+(v6+gamma)*v8
        go to 1440
1430  v8=(n+v5+v2)/(n*v6+v3)
        v9=(v4+alpha)+(v6+gamma)*v7
        v10=(beta+v5)+(v6+gamma)*v8
1440  v11=-v9/v10
        v12=v7+v8*v11
        v13=(h*alpha*v4-n*(e-f)*v1)/(n*(e-f)*v3-h*gamma*v6)
        v14=(h*beta*v5-n*(e-f)*v2)/(n*(e-f)*v3-h*gamma*v6)
        o=e-f
        if(a(2).lt.0.0) go to 1450
        a11=((n*o*v1+h*v4*alpha)*dsinh(alpha*bb)+(-n*o*v2*v11*
        *h*v5*beta*v11)*dsinh(beta*bb)+(-n*o*v3*v12+h*v6*v12*
        *gamma)*dsinh(gamma*bb))/1.d10
        a12=((n*o*v1+h*v4*alpha)*dcosh(alpha*bb)+
        *(-n*o*v3*v13+h*v6*v13*gamma)*dcosh(gamma*bb))/1.d10
        a13=((n*o*v2+h*v5*beta)*dcosh(beta*bb)+
        *(-n*o*v3*v14+h*v6*v14*gamma)*dcosh(gamma*bb))/1.d10
        a21=((v1*alpha+n*v4)*dcosh(alpha*bb)+
        *(v2*beta*v11+n*v5*v11)*dcosh(beta*bb)+
        *(v3*v12*gamma+n*v6*v12)*dcosh(gamma*bb))/1.d10
        a22=((v1*alpha+n*v4)*dsinh(alpha*bb)+
        *(v3*v13*gamma+n*v6*v13)*dsinh(gamma*bb))/1.d10
        a23=((v2*beta+n*v5)*dsinh(beta*bb)+
        *(v3*v14*gamma+n*v6*v14)*dsinh(gamma*bb))/1.d10
        a31=((v4+alpha)*dcosh(alpha*bb)+(v5*v11+beta*v11)*
        *dcosh(beta*bb)+(v6*v12+gamma*v12)*dcosh(gamma*bb))/1.d10
        a32=((v4+alpha)*dsinh(alpha*bb)+(v6*v13+gamma*v13)*
        *dsinh(gamma*bb))/1.d10
        a33=((v5+beta)*dsinh(beta*bb)+(v6*v14+gamma*v14)*
        *dsinh(gamma*bb))/1.d10
        go to 1460
1450  a11=((n*o*v1+h*v4*alpha)*dsinh(alpha*bb)+(-n*o*v2*v11*
        *h*v5*beta*v11)*dsin(beta*bb)+(-n*o*v3*v12+h*v6*v12*
        *gamma)*dsinh(gamma*bb))/1.d10
        a12=((n*o*v1+h*v4*alpha)*dcosh(alpha*bb)+
        *(-n*o*v3*v13+h*v6*v13*gamma)*dcosh(gamma*bb))/1.d10
        a13=((n*o*v2+h*v5*beta)*dcos(beta*bb)+
        *(-n*o*v3*v14+h*v6*v14*gamma)*dcosh(gamma*bb))/1.d10
        a21=((v1*alpha+n*v4)*dcosh(alpha*bb)+
        *(v2*beta*v11-n*v5*v11)*dcos(beta*bb)+
        *(v3*v12*gamma+n*v6*v12)*dcosh(gamma*bb))/1.d10
        a22=((v1*alpha+n*v4)*dsinh(alpha*bb)+
        *(v3*v13*gamma+n*v6*v13)*dsinh(gamma*bb))/1.d10
        a23=((v2*beta+n*v5)*dsin(beta*bb)+
        *(v3*v14*gamma+n*v6*v14)*dsinh(gamma*bb))/1.d10
        a31=((v4+alpha)*dcosh(alpha*bb)+(-v5*v11+beta*v11)*
        *dcos(beta*bb)+(v6*v12+gamma*v12)*dcosh(gamma*bb))/1.d10
        a32=((v4+alpha)*dsinh(alpha*bb)+(v6*v13+gamma*v13)*
        *dsinh(gamma*bb))/1.d10
        a33=((v5-beta)*dsin(beta*bb)+(v6*v14+gamma*v14)*
        *dsinh(gamma*bb))/1.d10
1460  det=a11*(a22*a33-a23*a32)-a12*(a21*a33-a31*a23)+*
        *a13*(a21*a32-a31*a22)
        go to 750
        stop

```

```

    end
    SUBROUTINE buckle(coeft4,coeft2,coeft0,r,n,
*e,f,g,h,z,sd)
c
c Subroutine to calculate coefficients of angle
c theta , for the buckling case
c
    COMMON /A/A44,D12,D66,D11,D22,m,aa
    REAL n
    INTEGER sd
    DOUBLE PRECISION coeft4,coeft2,coeft0,r,e,
*f,g,h,z,pi,aa
    pi=3.1415927
    if(sd.eq.1) go to 1910
    write(6,1900)
1900  format('you have removed shear deformation effects')
    write(6,1901)
1901  format('from the problem. You no longer have a cubic')
    write(6,1902)
1902  format('equation to solve so that the rest of this')
    write(6,1903)
1903  format('program is useless. An altogether different')
    write(6,1904)
1904  format('program would have to be used. Sorry!!!',/)
    return
1910  z=5./6.*A44
    e=D12+D66
    f=D66
    g=D11
    h=D22
    n=FLOAT(m)*pi/aa
    coeft4=-1.*(h*z*z+g*h*n*n*z+f*h*n*n*z+f*f*n*n*z-
*e*n*n*z-f*h*n*n*r)/(f*h*z)
    coeft2=-1.*(-2.*f*n*n*z*z-2.*e*n*n*z*z+h*n*n*r*z+
*f*n*n*r*z-g*h*z*n**4-f*g*z*n**4-f*f*z*n**4-
*e*e*z*n**4+g*h*r*n**4+f*f*n*n*r-e*e*r*n**4)/(f*h*z)
    coeft0=-1.*(-n*n*z*z*r-g*z*r*n**4-f*z*r*n**4-f*g*r*n**6
+g*z*z*n**4+f*g*r*n**6)/(f*h*z)
    return
    end
    SUBROUTINE vibes(coeft4,coeft2,coeft0,w,rho,thick,n,
*e,f,g,h,L,x,z,sd)
c
c Subroutine to calculate coefficients of angle
c theta, for the vibration case.
c
    COMMON /A/A44,D12,D66,D11,D22,m,aa
    REAL n
    INTEGER sd
    DOUBLE PRECISION coeft4,coeft2,coeft0,w,rho,thick,
*e,f,g,h,z,x,pi,aa
    if(sd.eq.1) go to 1960
    write(6,1950)
1950  format('you have just decided to remove all shear thru')
    write(6,1951)
1951  format('the thickness effects from this problem. The')
    write(6,1952)

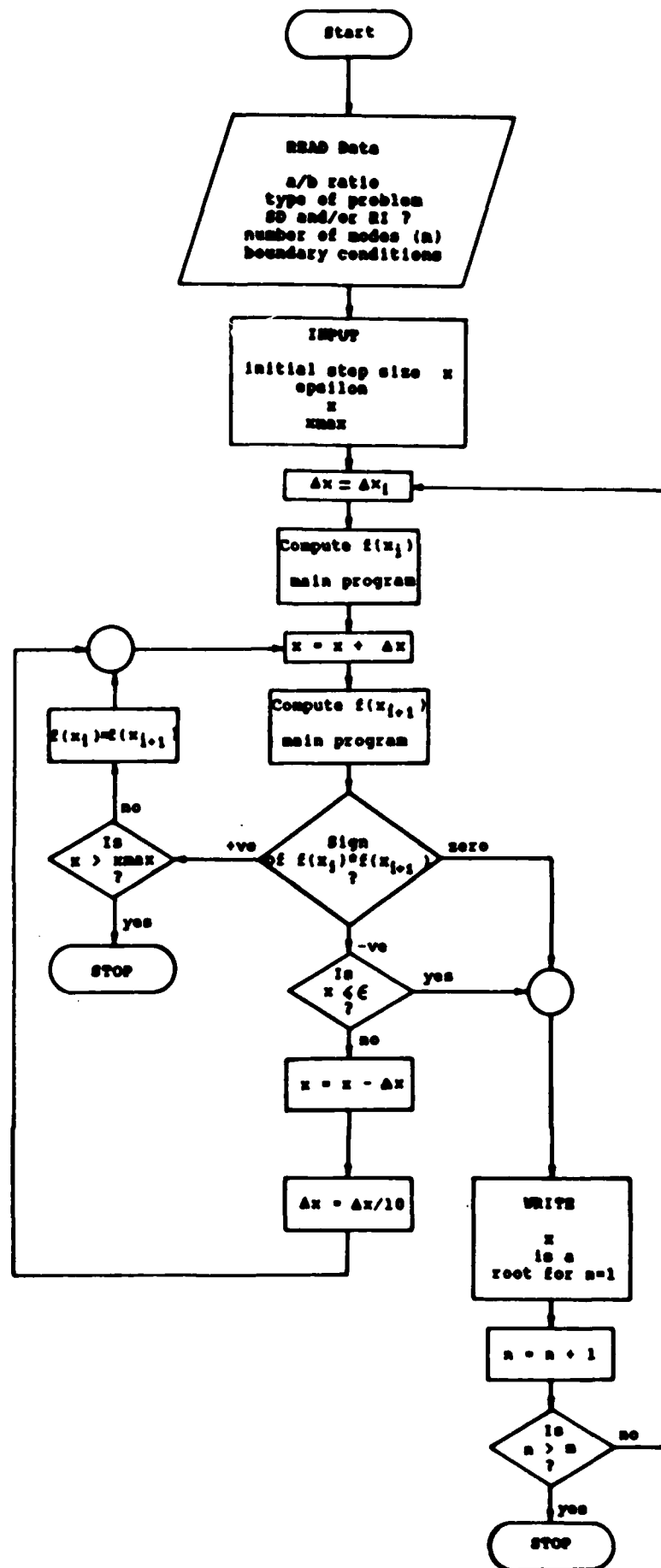
```

```

1952 format('program you are using is no longer valid as it is')
        write(6,1953)
1953 format('set up to solve a cubic. A totally different')
        write(6,1954)
1954 format('program would have to be used for this simpler')
        write(6,1955)
1955 format('case. So sorry old chap.',/)
        return
1960 z=5./6.*A44
        pi=3.1415927
        e=D12+D66
        f=D66
        g=D11
        h=D22
        if(L.eq.1) go to 2000
        x=0.0
        go to 2010
2000 x=w*w*rho*thick**3/(144.*32.174)
2010 y=rho*thick*w*w/(12.*32.174)
        n=FLOAT(m)*pi/aa
        coef4=(-h*z*z+h*x*z+f*x*z-g*h*n*n*z-f*h*n*n*z
        *-f*f*n*n*z+e*e*n*n*z+f*h*y)/(f*h*z)
        coef2=(-x*z*z+2.*f*f*n*n*z*z+2.*e*e*n*n*z*z-h*y*z-f*y*z
        *+x*x*z-h*n*n*x*z-g*n*n*x*z-2.*f*f*n*n*x*z+g*h*z*n**4
        *+f*g*z*n**4+f*f*z*n**4-e*e*z*n**4+h*x*x*y+f*x*x*y
        *-g*h*n*n*y-f*f*n*n*y+e*e*n*n*y)/(f*h*z)
        coef0=(y*z*z+n*n*x*z*z-g*z*z*n**4-2.*x*x*y*z+g*y*z*n*n
        *+f*f*n*n*y*z-n*n*x*x*z+g*x*x*z*n**4+f*x*x*z*n**4-f*g*z*n**6
        *+x*x*x*y-g*n*n*x*x*y-f*n*n*x*x*y+f*g*y*n**4)/(f*h*z)
        return
        end

```

Appendix E



BIBLIOGRAPHY

1. Brunelle, E.J., "Buckling of Transversely Isotropic Mindlin Plates", AIAA J., 9: 1018-1022 (1970).
2. Bowlus, J.A., The Determination of the Natural Frequencies and Mode Shapes for Anisotropic Laminated Plates Including the Effects of Shear Deformation and Rotary Inertia. MS Thesis. School of Engineering, Air Force Institute of Technology (AU), Wright-Patterson AFB OH, September 1985.
3. UNIX MACSYMA, release 309.2. 1976, 1984 Massachusetts Institute of Technology.
4. Dickson, L.E., New First Course in the Theory of Equations. New York: Wiley and Sons Company, 1948.
5. James, M.L., Smith, G.M., Walford, J.C., Applied Numerical Methods for Digital Computation (Second Edition), New York: Harper and Row, 1977.
6. Dawe, D.J., Craig, T.J., "The Influence of Shear Deformation on the Natural Frequencies of Laminated Rectangular Plates", Composite Structures, 3: 660-676 (1985).
7. Dawe, D.J., Craig, T.J., "The Vibration and Stability of Symmetrically Laminated Rectangular Plates Subjected to In Plane Stresses", Composite Structures, 5: 281-307 (1986).
8. Whitney, J.M., Structural Analysis of Laminated Anisotropic Plates. Lancaster, PA: Technomic Publishing Company, 1987.
9. Hildebrand F.B., Reissner E., Thomas G.B., "Notes on the Foundation of the Theory of Small Displacements of Orthotropic Shells", NACA: (1949).
10. Mindlin, R.D., "Influence of Rotary Inertia and Shear on Flexural Motions of Isotropic Elastic Plates", Journal of Applied Mechanics, 18: 31-38 (1951).
11. Yang, P.C., Norris, C.H., Stovsky, Y., "Elastic Wave Propagation in Heterogeneous Plates", International Journal of Solids and Structures, 2: 665-684 (1966).
12. Whitney, J.M., Pagano, N.J., "Shear Deformation in Heterogeneous Anisotropic Plates", J. of Applied Mechanics, 37: 1031-1036 (1970).
13. Timoshenko S. and Woinowsky-Krieger., Theory of Plates and Shells. New York: McGraw-Hill Book Company, 1959.
14. Reissner, E., "The Effect of Transverse Shear Deformation on the Bending of Elastic Plates", J. of Applied Mechanics, 12: 69-77 (1945).

15. Whitney, J.M., "Shear Correction Factors for Orthotropic Laminates Under Static Loading", J. of Applied Mechanics, 40: 302-304 (1973).
16. Craig, T.J., Dawe, D.J., "Flexural Vibration of Symmetrically Laminated Composite Rectangular Plates Including Transverse Shear Effects", International Journal of Solids and Structures, 22: 155-169 (1986).
17. Jones, R.M., Mechanics of Composite Materials. New York: McGraw-Hill Book Company, 1975.
18. Reddy, J.N., "Free Vibration of Antisymmetric Angle-Ply Laminated Plates Including Transverse Shear Deformation by the Finite Element Method", J. Sound and Vibration, 66: 565-576 (1979).
19. Reddy, J.N. and Others, "Vibration of Thick Rectangular Plates of Bimodulus Composite Material", Dept. of the Navy, Office of Naval Research, Contract #N00014-78-C-0647, Project NR 064-609 (1980).
20. Sathyamoorthy, M. and Chia, C.Y., "Effect of Transverse Shear and Rotary Inertia on Large Amplitude Vibration of Anisotropic Skew Plates", J. of Applied Mechanics, 47: 128-138 (1980).
21. Saada, Adel S. Elasticity Theory and Applications (Second Edition). Malabar Fl: Robert E. Krieger Publishing Company, 1983.
22. Sun, C.T., "Incremental Deformations in Orthotropic Laminated Plates Under Initial Stress", Transcript ASME, J. of Applied Mechanics, 34: 193-200 (1973).
23. Whitney, J.M., "The Effect of Transverse Shear Deformation on the Bending of Laminated Plates", J. of Composite Materials, 3: 534-547 (1969).
24. Dawe, D.J., and Roufaeil, O.L., "Buckling of Rectangular Mindlin Plates", Computers and Structures, 15: 461-471 (1982).
25. Pryor, C.W., and Barker, R.M., "A Finite Element Analysis Including Transverse Shear Effects for Applications to Laminated Plates", AIAA J., 9: 912-917 (1971).
26. Reddy, J.N. and Others, "Levy Type Solutions for Symmetrically Laminated Rectangular Plates Using First Order Shear Deformation Theory", Transactions of the ASME, 54: 740-742 (1987).
27. Leissa, A.W., "Buckling Laminated Composite Plates and Shells", Department of the Air Force, Flight Dynamics Laboratory, Contract #AFWAL-TR-85-3069 (1985).

VITA

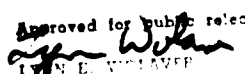
Joseph Real Francis Palardy was born on September 18, 1959 in the Montreal Children's Hospital, Quebec. He graduated from Macdonald-Carter Memorial High School in June 1976. He completed a two year program in pure and applied sciences at Champlain Regional College, located in Longueuil, before entering Concordia University in Montreal. After graduating with distinction from the mechanical engineering program in 1982, he joined the Canadian Armed Forces as he had been told, "there was no life like it". After completing a one year classification course in CFB Borden, Ontario, he was sent to Western Canada to serve a two year term as maintenance engineer at Canadian Forces Base Moose Jaw. He entered the School of Engineering, Air Force Institute of Technology, in June 1986.

Permanent address: Armament Dept/AETE
CFB Cold Lake
Cold Lake, Alberta

A18974

REPORT DOCUMENTATION PAGE

1a. REPORT SECURITY CLASSIFICATION Unclassified		1b. RESTRICTIVE MARKINGS None	
2a. SECURITY CLASSIFICATION AUTHORITY		3. DISTRIBUTION/AVAILABILITY OF REPORT Approved for public release; distribution unlimited.	
2b. DECLASSIFICATION/DOWNGRADING SCHEDULE		4. PERFORMING ORGANIZATION REPORT NUMBER(S)	
AFIT GAE AA 87D-16		5. MONITORING ORGANIZATION REPORT NUMBER(S)	
6a. NAME OF PERFORMING ORGANIZATION School of Engineering	6b. OFFICE SYMBOL (If applicable) AFIT ENY	7a. NAME OF MONITORING ORGANIZATION	
6c. ADDRESS (City, State, and ZIP Code) Air Force Institute of Technology Wright-Patterson Air Force Base OH 45433		7b. ADDRESS (City, State, and ZIP Code)	
8a. NAME OF FUNDING/SPONSORING ORGANIZATION	8b. OFFICE SYMBOL (If applicable)	9. PROCUREMENT INSTRUMENT IDENTIFICATION NUMBER	
8c. ADDRESS (City, State, and ZIP Code)		10. SOURCE OF FUNDING NUMBERS	
		PROGRAM ELEMENT NO.	PROJECT NO.
		TASK NO.	WORK UNIT ACCESSION NO.
11. TITLE (Include Security Classification)			
12. PERSONAL AUTHOR(S) Real F. Palardy, CPT, CAF			
13a. TYPE OF REPORT Ms Thesis	13b. TIME COVERED FROM _____ TO _____	14. DATE OF REPORT (Year, Month, Day) 1987 December	15. PAGE COUNT
16. SUPPLEMENTARY NOTATION			
17. COSATI CODES		18. SUBJECT TERMS (Continue on reverse if necessary and identify by block number)	
FIELD	GROUP	SUB-GROUP	
19. ABSTRACT (Continue on reverse if necessary and identify by block number)			
Thesis Advisor: Dr. Anthony Palazotto Department of Aeronautics and Astronautics			
ABSTRACT ON BACK			
20. DISTRIBUTION/AVAILABILITY OF ABSTRACT <input type="checkbox"/> UNCLASSIFIED/UNLIMITED <input checked="" type="checkbox"/> SAME AS RPT <input type="checkbox"/> DTIC USERS		21. ABSTRACT SECURITY CLASSIFICATION Unclassified	
22a. NAME OF RESPONSIBLE INDIVIDUAL Dr. Anthony Palazotto		22b. TELEPHONE (Include Area Code) (513) 255-3517	22c. OFFICE SYMBOL AFIT ENY

Approved for public release: IAW AFR 190-4

 LYNN E. WINKLER
 Director, Defense Information Systems Agency
 Defense Science and Technology Group
 Wright-Patterson Air Force Base, OH 45433-7777

19. ABSTRACT

An analytical study is conducted to determine the stability and free vibration characteristics of laminated anisotropic plates using the Levy approach. Included in the plate model are the effects of shear deformation and rotary inertia. Six different boundary conditions in the y direction are analyzed in conjunction with simply-supported boundaries in the x direction. The y directed boundaries considered are simple-simple, clamped-clamped, simple-clamped, simple-free, clamped-free, and free-free.

Solutions are presented for the buckling loads and natural frequencies of rectangular, graphite-epoxy symmetric plates. The results indicate the importance of including shear effects and rotary inertia in a plate's mathematical model. The overall importance of these equation parameters is definitely a function of the boundary condition and a general statement cannot be made. In addition, the effectiveness of the Levy technique, in studying laminated problems, becomes apparent in handling the more complicated boundaries as compared to the Galerkin or Rayleigh-Ritz techniques.

END

DATE

FILM

K-88

DTIC